# Studies of Reductive Elimination Reactions To Form Carbon−Oxygen Bonds from Pt(IV) Complexes

**B. Scott Williams and Karen I. Goldberg***

*Contribution from the Department of Chemistry, University of Washington, P.O. Box 351700, Seattle, Washington 98195-1700*

*Received September 13, 2000*

**Abstract:** The platinum(IV) complexes *fac*-$L_2PtMe_3(OR)$ ($L_2$ = bis(diphenylphosphino)ethane, *o*-bis(diphenylphosphino)benzene, R = carboxyl, aryl; L = $PMe_3$, R = aryl) undergo reductive elimination reactions to form carbon−oxygen bonds and/or carbon−carbon bonds. The carbon−oxygen reductive elimination reaction produces either methyl esters or methyl aryl ethers (anisoles) and $L_2PtMe_2$, while the carbon−carbon reductive elimination reaction affords ethane and $L_2PtMe(OR)$. Choice of reaction conditions allows the selection of either type of coupling over the other. A detailed mechanistic study of the reductive elimination reactions supports dissociation of the $OR^-$ ligand as the initial step for the C−O bond formation reaction. This is followed by a nucleophilic attack of $OR^-$ upon a methyl group bound to the Pt(IV) cation to produce the products MeOR and $L_2PtMe_2$. C−C reductive elimination proceeds from $L_2PtMe_3(OR)$ by initial L (L = $PMe_3$) or $OR^-$ ($L_2$ = dppe, dppbz) dissociation, followed by C−C coupling from the resulting five-coordinate intermediate. Our studies demonstrate that both C−C and C−O reductive elimination reactions from Pt(IV) are more facile in polar solvents, in the presence of Lewis acids, and for $OR^-$ groups that contain electron withdrawing substituents.

## Introduction

Reductive elimination is a key bond-forming and product-release step in homogeneous catalysis.[1] The formation of carbon−oxygen bonds by reductive elimination is a particularly powerful reaction as it can result in the production of alcohols, ethers, and esters. Despite the significance and potential importance of this reaction in both homogeneous catalysis[2−8] and interesting stoichiometric metal-mediated reactions,[9,10] only a limited number of examples of directly observed reductive elimination reactions which form C−O bonds from model complexes are known.[7,11−17] In addition, these latter reactions primarily occur at low-valent $d^8$ metal centers (such as Pd(II))[7,12−14] and/or involve aryl and acyl carbon groups.[7,12,13,15] Examples of C−O reductive elimination reactions involving alkyl carbons and higher oxidation state metals (e.g., Pd(IV), Pt(IV), Rh(III), and Ir(III)) are quite rare.[11,16−18]

However, the product release step in platinum-catalyzed alkane oxidation reactions is proposed to be such a C−O coupling reaction involving an alkyl group from a high-valent metal center.[3,4,19] Support has been presented for nucleophilic attack of water on a Pt(IV)-methyl group as the methanol-

(1) Parshall, G. W.; Ittel, S. D. *Homogeneous Catalysis: The Applications and Chemistry of Catalysis by Soluble Transition Metal Complexes*, 2nd ed.; Wiley-Interscience: New York, 1992.

(2) (a) Shilov, A. E. *Activation of Saturated Hydrocarbons by Transition Metal Complexes*; D. Riedel: Dordrecht, The Netherlands, 1984. (b) Shilov, A. E.; Shul'pin, G. B. *Chem. Rev.* **1997**, *97*, 10235.

(3) Stahl, S. S.; Labinger, J. A.; Bercaw, J. E. *Angew. Chem., Int. Ed.* **1998**, *37*, 2180 and references therein.

(4) Periana, R. A.; Taube, D. J.; Gamble, S.; Taube, H.; Satoh, T.; Fujii, H. *Science* **1998**, *280*, 560.

(5) (a) Sen, A. *Acc. Chem. Res.* **1988**, *21*, 421. (b) Sen, A. *Acc. Chem. Res.* **1998**, *31*, 550.

(6) (a) Mann, G.; Hartwig, J. F. *Tetrahedron Lett.* **1997**, *38*, 8005. (b) Mann, G.; Hartwig, J. F. *J. Org. Chem.* **1997**, *62*, 5413.

(7) (a) Mann, G.; Hartwig, J. F. *J. Am. Chem. Soc.* **1996**, *118*, 13109. (b) Hartwig, J. F. *Angew. Chem., Int. Ed. Engl.* **1998**, *37*, 2046 and references therein. (c) Hartwig, J. F. *Acc. Chem. Res.* **1998**, *31*, 852. (d) Mann, G.; Incarvito, C.; Rheingold, A. L.; Hartwig, J. F. *J. Am. Chem. Soc.* **1999**, *121*, 3224.

(8) (a) Palucki, M.; Wolfe, J. P.; Buchwald, S. L. *J. Am. Chem. Soc.* **1996**, *118*, 10333. (b) Palucki, M.; Wolfe, J. P.; Buchwald, S. L. *J. Am. Chem. Soc.* **1997**, *119*, 3395. (c) Aranyos, A.; Old, D. W.; Kiyomori, A.; Wolfe, J. P.; Sadighi, J. P.; Buchwald, S. L. *J. Am. Chem. Soc.* **1999**, *121*, 4369.

(9) (a) Davidson, M. F.; Grove, D. M.; van Koten, G.; Spek, A. L. *J. Chem. Soc., Chem. Commun.* **1989**, 1562. (b) Kapteijn, G. M.; Dervisi, A.; Verhoef, M. J.; van den Broek, M. A. F. H.; Grove, D.; van Koten, G. *J. Organomet. Chem.* **1996**, *517*, 123.

(10) (a) Bernard, K. A.; Atwood, J. D. *Organometallics* **1987**, *6*, 1133. (b) Bernard, K. A.; Atwood, J. D. *Organometallics* **1988**, *7*, 235. (c) Bernard, K. A.; Atwood, J. D. *Organometallics* **1989**, *8*, 795. (d) Bernard, K. A.; Churchill, M. R.; Janik, T. S.; Atwood, J. D. *Organometallics* **1990**, *9*, 12.

(11) Thompson, J. S.; Randall, S. L.; Atwood, J. D. *Organometallics* **1991**, *10*, 3906. See ref 7a for more information on this reaction.

(12) (a) Widenhoefer, R. A.; Zhong, H. A.; Buchwald, S. L. *J. Am. Chem. Soc.* **1997**, *119*, 6787. (b) Widenhoefer, R. A.; Buchwald, S. L. *J. Am. Chem. Soc.* **1998**, *120*, 6504 and references therein.

(13) Komiya, S.; Akai, Y.; Tanaka, K.; Yamamoto, T.; Yamamoto, A. *Organometallics* **1985**, *4*, 1130.

(14) (a) Koo, K.; Hillhouse, G. L. *Organometallics* **1998**, *17*, 2924. (b) Han, R.; Hillhouse, G. L.; *J. Am. Chem. Soc.* **1997**, *119*, 8135. (c) Matsunaga, P. T.; Mavropoulos, J. C.; Hillhouse, G. L. *Polyhedron* **1995**, *14*, 175. Note that since these reductive elimination reactions from Ni(II) are promoted by oxidants, Ni(III) is likely to be involved in the reactions.

(15) Haarman, H. F.; Kaagman, J.-W. F.; Smeets, W. J. J.; Spek, A. L.; Vrieze, K. *Inorg. Chim. Acta* **1998**, *270*, 34.

(16) (a) Canty, A. J.; Jin, H. *J. Organomet. Chem.* **1998**, *565*, 135. (b) Canty, A. J.; Jin, H.; Skelton, B. W.; White, A. H. *Inorg. Chem.* **1998**, *37*, 3975.

(17) For a preliminary report on C−O reductive elimination of methyl esters from Pt(IV), see: Williams, B. S.; Holland, A. W.; Goldberg, K. I. *J. Am. Chem. Soc.* **1999**, *121*, 252.

(18) The reverse of alkyl C−O reductive elimination, alkyl C−O oxidative addition, has been observed. (a) Ittel, S. D.; Tolman, C. A.; English, A. D.; Jesson, J. P. *J. Am. Chem. Soc.* **1978**, *100*, 7577. (b) Tolman, C. A.; Ittel, S. D.; English, A. D.; Jesson, J. P. *J. Am. Chem. Soc.* **1979**, *101*, 1742. (c) van der Boom, M. E.; Liou, S. Y.; Ben-David, Y.; Vigalok, A.; Milstein, D. *J. Am. Chem. Soc.* **1998**, *120*, 6531.

10.1021/ja003366k CCC: $20.00 
Published on Web 02/23/2001

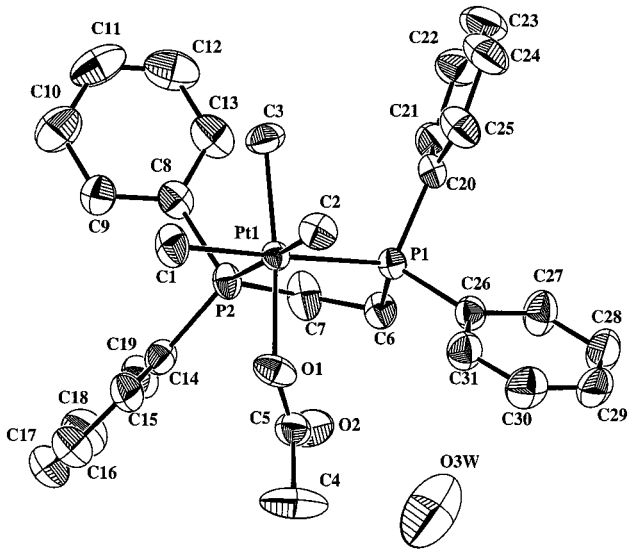


**Figure 1.** ORTEP diagram of *fac*-(dppe)$PtMe_3OAc$ (**1a**). Ellipsoids are shown at the 50% probablity level. Hydrogens are omitted for clarity.

forming step in Shilov's original Pt-catalyzed oxidations.[3,19] Similarly, the reductive elimination of a methyl and a sulfonate group from Pt(IV) has been proposed as the methylbisulfate forming step in the recently reported Catalytica methane oxidation reaction.[4] Such carbon−oxygen bond formation to release the alcohol in a protected form such as an ester or sulfonate ester has been advanced as a useful strategy to avoid the overoxidation of the desired alcohol to carbon dioxide and water, a significant problem in selective alkane oxidation catalysis.[3−5]

Detailed investigations of a variety of alkyl C−O reductive elimination reactions from Pt(IV), including those which form esters, have now been carried out.[17] Thermolyses of the Pt(IV) complexes, *fac*-$L_2PtMe_3OR$ ($L_2$ = bis(diphenylphosphino)ethane (dppe), *o*-bis(diphenylphosphino)benzene (dppbz), R = carboxyl, aryl; L = $PMe_3$, R = aryl), under the proper conditions produce high yields of methyl esters and methyl aryl ethers. Kinetic and mechanistic studies of these novel C−O reductive elimination reactions from Pt(IV) have allowed us to identify trends and requirements for both the neutral ligands on the metal and the oxygen groups involved in the coupling reactions.

## Results

**Platinum(IV) Carboxylates.** The Pt(IV) acetate complex *fac*-(dppe)$PtMe_3$(OAc) (**1a**) was prepared by reaction of *fac*-(dppe)-$PtMe_3I$ with AgOAc in toluene at room temperature. Complex **1a** has been characterized by spectroscopy, elemental analysis, and X-ray crystallography. The ORTEP diagram appears in Figure 1 and selected bond lengths and angles are presented in Table 1.[20] The crystal was grown by slow evaporation of a toluene solution of **1a** in ambient air, and contains a water molecule hydrogen bound to the acetate moiety (O−O distance = 2.7 Å). A slightly distorted octahedral geometry is observed about the platinum center, and the Pt(IV) carbon and phosphorus bond lengths are comparable to those in other reported structures with similar trans ligands.[21] The Pt−O bond length in **1a** (2.159(4) Å) is the longest of the Pt(IV) acetate complexes which have been structurally characterized, including several cases in which the acetate is involved in hydrogen bonding.[22] In addition, the formal carbon−oxygen single and double bonds in the acetate fragment have very similar bond lengths (1.268(8) and 1.229(8) Å), suggesting that the carboxylate $\pi$-bond is rather delocalized and the bonding to platinum fairly ionic. Two strong carboxylate stretches are observed in the IR spectrum of **1a** ($CH_2Cl_2$) at 1614 and 1377 $cm^{-1}$. The small difference between the asymmetric and symmetric stretches ($\Delta$ = 237 $cm^{-1}$) is also indicative of significant ionic bonding.[23]

**Table 1.** Selected Bond Lengths and Angles in the Crystal Structure of **1a**

| bond lengths (Å) | | bond angles (deg) | |
|---|---|---|---|
| Pt−C(1) | 2.103(6) | P(1)−Pt−P(2) | 83.67(5) |
| Pt−C(2) | 2.087(6) | C(1)−Pt−C(2) | 84.5(3) |
| Pt−C(3) | 2.080(6) | C(1)−Pt−P(2) | 95.7(2) |
| Pt−P(1) | 2.3793(15) | C(2)−Pt−P(1) | 96.02(18) |
| Pt−P(2) | 2.3767(16) | C(3)−Pt−P(1) | 93.6(2) |
| Pt−O(1) | 2.159(4) | C(3)−Pt−P(2) | 92.31(19) |
| O(1)−C(5) | 1.268(8) | C(3)−Pt−C(1) | 84.4(3) |
| O(2)−C(5) | 1.229(8) | C(3)−Pt−C(2) | 86.7(3) |
| C(5)−C(4) | 1.501(9) | O(1)−Pt−P(1) | 96.72(13) |
| C(6)−P(1) | 1.842(6) | O(1)−Pt−P(2) | 97.01(12) |
| C(7)−P(2) | 1.858(6) | O(1)−Pt−C(1) | 85.3(2) |
| C(6)−C(7) | 1.539(9) | O(1)−Pt−C(2) | 84.0(2) |
| O(2)−O(3W) | 2.7 | Pt−O(1)−C(5) | 125.3(4) |
| | | O−(1)-C(5)−C(4) | 115.8(6) |
| | | O(1)−C(5)−O(2) | 124.8(6) |
| | | O(2)−C(5)−C(4) | 119.4(6) |
| | | C(3)−Pt−O(1) | 166.8(2) |
| | | P(1)−Pt−C(1) | 178.0(2) |
| | | P(2)−Pt−C(2) | 178.95(17) |

Anhydrous samples of **1a** were prepared by recrystallization from toluene and pentane under air- and moisture-free conditions. The thermolyses of anhydrous samples of **1a** at 99 °C were studied in a variety of solvents. Competitive reductive elimination was observed, in which either a carbon−oxygen bond was formed to produce methyl acetate and (dppe)$PtMe_2$ (**2a**) or a carbon−carbon bond was formed to produce ethane and (dppe)PtMe(OAc)[24] (**3a**) (Scheme 1). There is a strong

(19) Nucleophilic attack by a heteroatom group ($X^-$) upon a metal-bound R group is sometimes classified as a reductive elimination as it results in C−X bond formation and a two oxidation state reduction of the metal. See: Collman, J. P.; Hegedus, L. S.; Norton, J. R.; Finke, R. G. *Principles and Applications of Organotransition Metal Chemistry*; University Science Books: Mill Valley, CA, 1987; pp 279−281. See ref 3 and references therein for more information about this form of C−O coupling at Pt(IV) centers.

(20) See Supporting Information for a complete listing of bond lengths and angles, atomic coordinates, and displacement parameters. Further refinement has been carried out on the crystal structure data after a preliminary report in ref 17.

(21) (a) Clark, H. C.; Ferguson, G.; Jain, V. K.; Parvez, M. *J. Organomet. Chem.* **1984**, *270*, 365. (b) O'Reilly, S. A.; White, P. S.; Templeton, J. L. *J. Am. Chem. Soc.* **1996**, *118*, 5684. (c) Redina, L. M.; Vittal, J. J.; Puddephatt, R. J. *Organometallics* **1995**, *14*, 2188. (d) Levy, C. J.; Vittal, J. J.; Puddephatt, R. J. *Organometallics* **1996**, *15*, 2108 (e) Hill, G. S.; Vittal, J. J.; Puddephatt, R. J. *Organometallics* **1997**, *16*, 1209. (f) Schlecht, S.; Magull, J.; Fenske, D.; Dehnicke, K. *Angew. Chem., Int. Ed. Engl.* **1997**, *36*, 1994. (g) Cheetham, A. K.; Puddephatt, R. J.; Zalkin, A.; Templeton, D. H.; Templeton, L. K. *Inorg. Chem.* **1976**, *15*, 2997. (h) Monojlovic-Muir, L.; Muir, K. W. *Croat. Chem. Acta* **1984**, *57*, 587. (k) Ling, S. S. M.; Jobe, I. R.; Monojlovic-Muir, L.; Muir, K. W.; Puddephatt, R. J. *Organometallics* **1985**, *4*, 1198. (l) Ling, S. S. M.; Payne, N. C.; Puddephatt, R. J. *Organometallics* **1985**, *4*, 1546. (m) Hoover, J. F.; Stryker, J. M. *Organometallics* **1989**, *8*, 2973.

(22) (a) Lee, E. J.; Jun, M.-J.; Lee, S. S.; Sohn, Y. S. *Polyhedron* **1997**, *16*, 2421. (b) Kratochwil, N. A.; Zabel, M.; Range, K.-J.; Bednarski, P. J. *J. Med. Chem.* **1996**, *39*, 2499. (c) Rochon, F. D.; Melanson, R.; Macquet, J.-P.; Belanger-Gariepy, F.; Beauchamp, A. L. *Inorg. Chim. Acta* **1985**, *108*, 17. (d) Ellis, L. T.; Er, H. M.; Hambley, T. W. *Aust. J. Chem.* **1995**, *48*, 793. (e) Neidle, S.; Snook, C. F.; Murrer, B. A.; Barnard, C. F. J. *Acta Crystallogr., Sect. C* **1995**, *C51*, 822. (f) Khokhar, A. R.; Deng, Y. *Inorg. Chim. Acta* **1993**, *204*, 35.

(23) Nakmoto, K. *Infrared and Raman Spectra of Inorganic and Coordination Compounds. Part B: Applications in Coordination, Organometallic and Bioinorganic Chemistry*, 5th ed.; John Wiley and Sons: New York, 1977; pp 59−62.

**Table 2.** Rate Constants and Product Yields for the Thermolysis of **1a** (99 °C)

| solvent | polarity[a] | $k_{obs}$ ($10^5$ $s^{-1}$) | % C−O | $k_{CO}$ ($10^5$ $s^{-1}$)[c] | % C−C | $k_{CC}$ ($10^5$ $s^{-1}$)[c] |
|---|---|---|---|---|---|---|
| $C_6D_6$ | 0.73 | 1.25 ± 0.04 | 88−89 (94−98[b]) | 1.17 ± 0.07 | 2−12 | 0.07 ± 0.04 |
| THF-$d_8$ | 0.84 | 1.28 ± 0.03 | 88 (96[b]) | 1.16 ± 0.07 | 4−12 | 0.12 ± 0.06 |
| acetone-$d_6$ | 1.06 | 60−110 | 1−5 | 2−4 | 95−99 | 60−110 |
| $C_6D_5NO_2$ | 1.14 | 140 ± 10 | <0.5 | *d* | 99.5+ | 140 ± 10 |

[a] Relative polarity scale for protio solvents.[25] [b] PVP added to the reaction (see text). [c] Reference 26. [d] Insufficient product was generated to accurately determine the rate constant.

**Scheme 1**

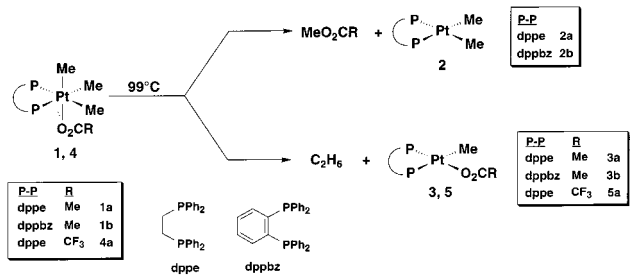


solvent dependence of the product ratios (C−O versus C−C coupling) and the rate constants for these reactions (Table 2).

In the relatively nonpolar solvents of $C_6D_6$ and THF-$d_8$, carbon−oxygen bond formation is favored with methyl acetate and **2a** as the primary products (88−89%). Even higher yields of C−O coupling products (94−98%) were observed when 2% cross-linked 4-polyvinylpyridine (PVP), a known acid scavenger, was added to the reaction. The fluorinated analogue, *fac*-(dppe)$PtMe_3(O_2CCF_3)$ (**4a**), prepared from *fac*-(dppe)$PtMe_3I$ and $AgO_2CCF_3$, undergoes a similar competitive reductive elimination at 99 °C in $C_6D_6$ to form either methyl trifluoroacetate and **2a** or ethane and (dppe)$PtMe(O_2CCF_3)$ (**5a**) (Scheme 1). However, the percentage of C−O coupled products in the presence of PVP in $C_6D_6$ was significantly lower for **4a** (49 ± 2%) than for **1a**. Yet, the overall reaction rate was considerably faster for **4a** than for **1a** ($k_{obs} = (2.9 \pm 0.1) \times 10^{-4}$ $s^{-1}$, as compared to $k_{obs} = (1.25 \pm 0.4) \times 10^{-5}$ $s^{-1}$ for **1a**). From the ratio of the products (**2a** to **3a** or **5a**), it can be determined that the rate constant for carbon−oxygen reductive elimination is 12 times faster for the more electron withdrawing trifluoroacetate compound, **4a**, than for the acetate complex, **1a**.[26] The rate constant for carbon−carbon coupling is 2 orders of magnitude faster for **4a** than for **1a**.

In contrast to the reactivity in the relatively nonpolar solvents $C_6D_6$ and THF-$d_8$, in which C−O coupling dominates, thermolysis of **1a** in the more polar solvents acetone-$d_6$ or nitrobenzene-$d_5$ favors carbon−carbon coupling (95−99% and 99+%, respectively). The rates of reductive elimination are also on the order of 2 to 3 orders of magnitude more rapid in these polar solvents (Table 2). It should also be noted that while the thermolysis of **1a** in acetone-$d_6$ consistently followed first-order kinetic behavior, a high variability in the rate constant was observed (at 99 °C, $k_{obs} = (6.2-11) \times 10^{-4}$ $s^{-1}$).[27] The exact cause of this variability is unclear.[28,29] However, when a constant acetate concentration was maintained by the addition of acetate ions as $[N(n\text{-}Bu)_4]OAc$ (0.38 or 0.60 M), a reproducible reaction rate independent of the acetate concentration was observed ($k_{obs} = (4.0 \pm 0.1) \times 10^{-5}$ $s^{-1}$).[30,31] Under these conditions, ethane production was completely inhibited and methyl acetate and (dppe)$PtMe_2$ (**2a**) were formed in quantitative yield. Thus, the carbon−oxygen bond formation rate constant in acetone-$d_6$ ($4.0 \times 10^{-5}$ $s^{-1}$) is approximately 4-fold the C−O coupling rate constant in the less polar solvents $C_6D_6$ and THF-$d_8$ ($1.1 \times 10^{-5}$ $s^{-1}$).

To investigate the effect of modification of the ancillary ligand, $L_2$, the analogous dppbz (*o*-bis(diphenylphosphinobenzene)) complex, *fac*-(dppbz)$PtMe_3(OAc)$ (**1b**), was prepared and its thermal reactivity studied. In the presence of PVP in THF-$d_8$ at 99 °C, **1b** undergoes reductive elimination to form primarily methyl acetate and (dppbz)$PtMe_2$ (**2b**) (94%) ($k_{obs} = 1.0 \times 10^{-5}$ $s^1$, $k_{CO} = 0.9 \times 10^{-5}$ $s^{-1}$), with carbon−carbon reductive elimination to form ethane and (dppbz)PtMe(OAc) (**3b**) representing a minor reaction ($k_{CC}$ = ca. $1 \times 10^{-6}$ $s^{-1}$) (Scheme 1). In the absence of added PVP, higher amounts of C−C coupling from **1b** were observed, as was the case for **1a**. When $[N(n\text{-}Bu)_4]OAc$ was added to the reaction, no carbon−carbon coupling was observed. The observed rate of C−O reductive elimination from **1b** was also independent of the amount of $[N(n\text{-}Bu)_4]OAc$ that was added to the reaction (20 mM $[N(n\text{-}Bu)_4]OAc$, $k_{obs} = k_{CO} = 1.2 \times 10^{-5}$ $s^{-1}$; 48 mM $[N(n\text{-}Bu)_4]OAc$, $k_{obs} = k_{CO} = 1.1 \times 10^{-5}$ $s^{-1}$). It should be noted that the rate constant for CO coupling for **1b** in THF-$d_8$ is virtually identical to that for the dppe analogue **1a** ($k_{CO} = 1.2 \times 10^{-5}$ $s^{-1}$).

**Effect of Lewis Acids.** Consistent with the observation that the addition of the acid scavenger, PVP, resulted in a retardation of C−C reductive elimination from the platinum acetate complexes **1a** and **1b**, addition of acids to the thermolysis reactions of **1a** caused a striking acceleration of the carbon−carbon coupling rate. In $C_6D_6$, the half-life of thermolysis of **1a** is approximately 15 h at 99 °C, forming primarily C−O products (90%). However, in the presence of even a small amount of triflic acid (0.1 equiv, 3 mM) or silver triflate (0.1 equiv, 6 mM), a dramatic change in reactivity occurred. Under these conditions, the C−C coupling products were produced exclusively at *room temperature* over the course of a day.

(24) **3a** and (dppe)$PtMe(CD_2COCD_3)$: Appleton, T. G.; Bennett, M. A. *Inorg. Chem.* **1978**, *17*, 938.

(25) Swain, C. G.; Swain, M. S.; Powell, A. L.; Alunni, S. *J. Am. Chem. Soc.* **1983**, *105*, 502.

(26) The rate constant for C−O reductive elimination is defined as follows: $k_{co}$ = (percent C−O products formed)($k_{obs}$)/100. Similarly, $k_{cc}$ = (percent C−C products formed)($k_{obs}$)/100 so that $k_{obs} = k_{CO} + k_{CC}$.

(27) A similar variation in rates was observed at 79 °C ($k_{obs} = (3.4-19) \times 10^{-5}$ $s^{-1}$).

(28) Possible sources of variability in $k_{obs}$(acetone-$d_6$): (a) Trace amounts of a Lewis acidic impurity could cause erratic kinetic behavior (see Results under Effect of Lewis Acids). (b) The acetone reactions may not be strictly first order. In contrast to thermolysis in less polar solvents, >95% of the reaction proceeds via C−C reductive elimination, which is inhibited by acetate ions (see text). The acetate concentration is a complex function of the concentration of **1a**, that of the major product, (dppe)PtMe(OAc) (**3a**), and of any acetic acid produced.[29]

(29) A side reaction between the primary Pt(II) product, (dppe)PtMe(OAc) (**3**), and acetone-$d_6$ to form (dppe)$PtMe(CD_2COCD_3)$[24] and DOAc further complicates the analysis. However, production of acetic acid during the reaction would be expected to cause a deviation from first-order behavior (see Results under Effect of Lewis Acids) rather than simple variability between experiments.

(30) The disappearance of starting material was monitored by $^1H$ NMR for two half-lives, beyond which, the dynamic range of the NMR spectrometer hindered accurate data collection.

(31) During the course of the thermolysis reaction, conversion of $[N(n\text{-}Bu)_4]OAc$ to $(n\text{-}Bu)_3N$ and *n*-BuOAc occurs at a rate approximately an order of magnitude slower than the Pt(IV) reductive eliminations.

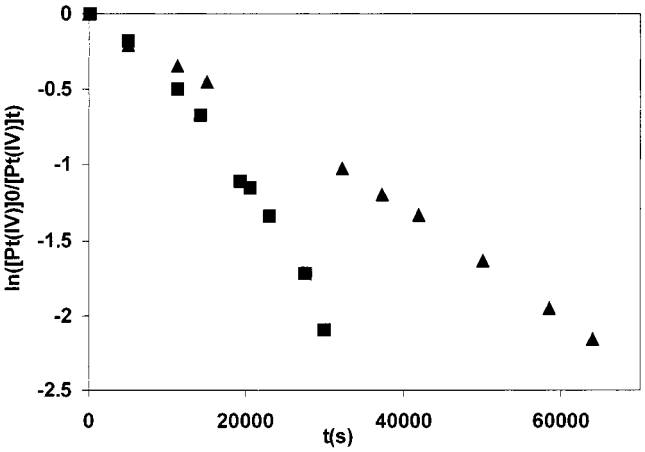


**Figure 2.** Curved first-order kinetic plots of the thermolysis of *fac*-(dppe)$PtMe_3$(*p*-$OC_6H_4Me$) (**6a**) at 120 °C (■ = $C_6D_6$, ▲ = THF-$d_8$).

**Scheme 2**

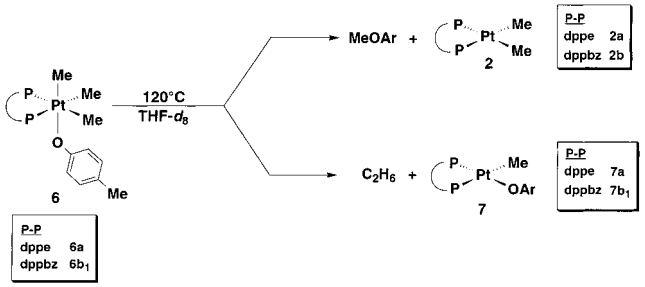


The addition of acetic rather than triflic acid to a $C_6D_6$ solution of **1a** afforded a rather different result. The initial ethane formation rate constant at 99 °C ($k_{CC}$ = ca. $5 \times 10^{-6}$ $s^{-1}$)[26] was clearly faster than that without added acid (ca. $1 \times 10^{-6}$ $s^{-1}$), yet the acceleration was much less pronounced than with triflic acid. Also unlike the triflic acid reaction, the primary products were the C−O coupling products, (dppe)$PtMe_2$ (**2a**) and methyl acetate (ca. 80%). Thus, the initial rate constant of methyl acetate production ($k_{CO}$ = $2.2 \times 10^{-5}$ $s^{-1}$) was approximately double that of the rate constant without acetic acid. However, as the reaction proceeded, the product **2a** itself reacted with the acetic acid to form (dppe)PtMe(OAc) (**3a**) and $CH_4$,[32] and the reaction approached its uncatalyzed product ratio and rate constant (ca. 90% C−O coupling and $k_{obs}$ = ca. $1.2 \times 10^{-5}$ $s^{-1}$).

**Platinum(IV) Aryloxides: (a) Platinum(IV) Aryloxide Complexes of dppe.** The complex *fac*-(dppe)$PtMe_3$(*p*-$OC_6H_4$-Me) (**6a**) was prepared in good yield (81%) by the reaction of *fac*-(dppe)$PtMe_3(O_2CCF_3)$ (**4a**) with potassium *p*-cresolate in THF at −78 °C and characterized by $^1H$, $^{13}C$, and $^{31}P$ NMR spectroscopy and elemental analysis. Thermolysis of **6a** in the relatively nonpolar solvent THF-$d_8$ at 120 °C afforded primarily the carbon−oxygen coupling products *p*-methylanisole and (dppe)$PtMe_2$ (**2a**) (ca. 85%). The carbon−carbon coupling products, ethane and (dppe)PtMe(*p*-$OC_6H_4Me$) (**7a**), made up the remaining fraction (ca. 15%) (Scheme 2). However, linear first-order kinetic behavior was not observed in these thermolyses of **6a** in THF-$d_8$ or in similar reactions carried out in $C_6D_6$ (Figure 2). Instead, the reactions accelerated as they progressed. As noted by the curvature in the plots in Figure 2, this accelerative behavior is more apparent in $C_6D_6$ than in THF-$d_8$. While accurate rate constant data could not be obtained from these nonlinear plots, the initial observed rate constants in both solvents were approximately $3 \times 10^{-5}$ $s^{-1}$.

(32) The reaction between **2a** and acetic acid was demonstrated independently.

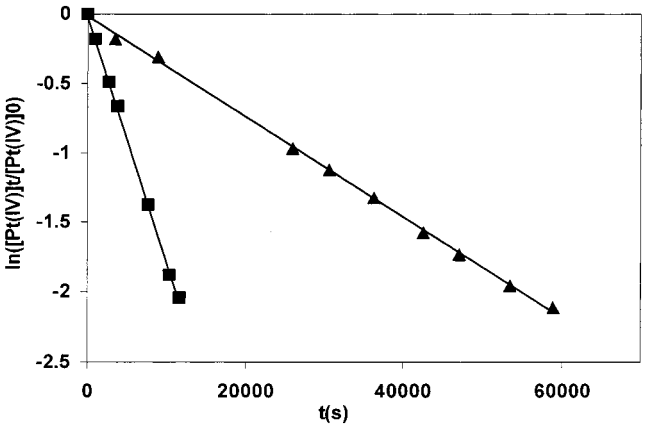


**Figure 3.** First-order kinetic plots of the thermolyses of *fac*-(dppe)-$PtMe_3$(*p*-$OC_6H_4Me$) (**6a**) at 120 °C with added aryloxide sources (■ = *p*-cresol, ▲ = [18-crown-6-potassium][*p*-cresolate]).

**Scheme 3**

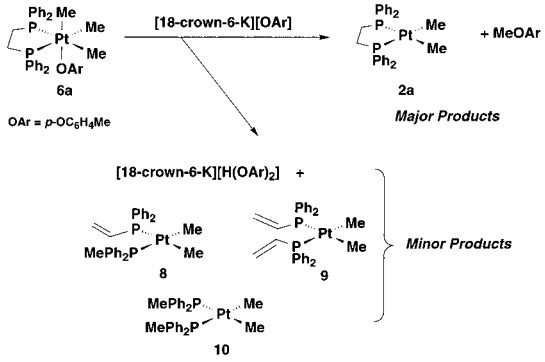


Addition of *p*-cresol (0.6 equiv, 18 mM) to the thermolysis of **6a** in THF-$d_8$ caused a substantial increase in reaction rate, but also resulted in linear first-order behavior ($k_{obs}$ = $1.77 \times 10^{-4}$ $s^{-1}$, 85% C−O coupling, $k_{CO}$ = ca. $1.5 \times 10^{-4}$ $s^{-1}$) (Figure 3). Addition of the conjugate base, [18-crown-6-K][*p*-$OC_6H_4$-Me], also produced linear first-order behavior ($k_{obs}$ = $3.61 \times 10^{-5}$ $s^{-1}$, 93% yield of methyl acetate) (Figure 3). However, in this latter thermolysis reaction, other side products were observed. The first of these side products was indicated by a broad singlet at ca. 17 ppm which is assigned to the bicresolate anion H[*p*-$OC_6H_4Me]_2^-$.[33] An additional series of signals, just visible above the baseline of the $^1H$ and $^{31}P$ NMR spectra, are assigned to the species *cis*-($PMePh_2$)($P(CHCH_2)Ph_2$)$PtMe_2$ (**8**), *cis*-$(P(CHCH_2)Ph_2)_2PtMe_2$ (**9**), and *cis*-$(PMePh_2)_2PtMe_2$ (**10**) (Scheme 3).

While **8**−**10** are minor side products when generated by the addition of a relatively mild base such as cresolate to dppe complexes, compounds **8**−**10** can also be quantitatively generated in THF by the reaction of *fac*-(dppe)$PtMe_3(O_2CCF_3)$ (**4a**) with the strong base KOH. This high-yield production of **8**−**10** allowed us to identify and characterize these complexes via $^1H$, $^{31}P\{^1H\}$, $^1H\{^{31}P\}$, $^1H$ COSY, and $^1H/^{31}P$ HELCO NMR experiments.[34] Complex **8** was the major product at early reaction times, but the distribution between **8**, **9**, and **10** reached a statistical 2:1:1 pattern over the course of the reaction as a result of phosphine exchange.[35] Subsequently, dppe was added to the reaction mixture, which cleanly generated (dppe)$PtMe_2$

(33) The chemical shift of this species varied between 16.5 and 17.5 ppm dependent upon the individual thermolysis reaction and the extent of reaction within the thermolysis. The same $^1H$ NMR signal was generated when *p*-cresol was added to [18-crown-6-K][*p*-$OC_6H_4Me$].

(34) HEteronuclear Long-range COrellation.

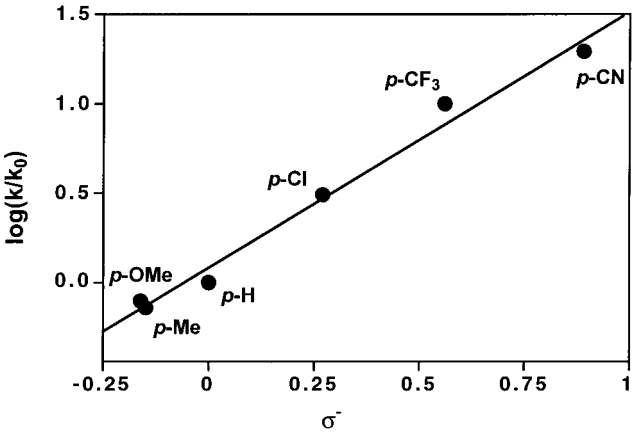


**Figure 4.** Hammett plot for the thermolysis of $\mathbf{6b_{1-6}}$ in THF-$d_8$ at 120 °C in the presence of [18-crown-6-potassium][OAr $^-$].

**Table 3.** Observed Rate Constants and $\sigma^-$ Values for Thermolyses of $\mathbf{6b_{1-6}}$ in THF-$d_8$ at 120 °C in the Presence of [18-Crown-6-potassium][OAr $^-$]

| complex | *p*-X | $\sigma^-$ | $k_{obs}$ ($10^5$ s$^{-1}$) |
|---|---|---|---|
| $\mathbf{6b_1}$ | Me | −0.15 | 2.05 |
| $\mathbf{6b_2}$ | H | 0.00 | 2.85 |
| $\mathbf{6b_3}$ | OMe | −0.16 | 2.22 |
| $\mathbf{6b_4}$ | Cl | +0.27 | 8.92 |
| $\mathbf{6b_5}$ | $CF_3$ | +0.56 | 28.7 |
| $\mathbf{6b_6}$ | CN | +0.89 | 56.2 |

(**2a**), $PPh_2Me$, and $PPh_2(CHCH_2)$, all of which had spectral characteristics that matched those of authentic samples.

**(b) Aryloxide Complexes of dppbz.** The aryloxide complex *fac*-(dppbz)$PtMe_3$(*p*-$OC_6H_4Me$) ($\mathbf{6b_1}$, dppbz = *o*-bis-(diphenylphosphino)benzene) was prepared by reaction of $[PtMe_3(OTf)]_4$ with potassium *p*-cresolate followed by the addition of dppbz (70% yield). The complex was characterized by $^1$H, $^{13}$C, and $^{31}$P NMR spectroscopy and elemental analysis. When $\mathbf{6b_1}$ was heated in THF-$d_8$ at 120 °C in the presence of PVP, *p*-methylanisole and (dppbz)$PtMe_2$ (**2b**) were the major products (92%), with the remainder being the C−C coupling products ethane and (dppbz)PtMe(*p*-$OC_6H_4Me$) ($\mathbf{7b_1}$) (Scheme 2).[36] In contrast to the thermolysis reactions of the dppe analogue, *fac*-(dppe)$PtMe_3$(*p*-$OC_6H_4Me$) (**6a**), the thermolysis of $\mathbf{6b_1}$ obeyed clean first-order kinetics through greater than three half-lives ($k_{obs} = (2.7 \pm 0.2) \times 10^{-5}$ s$^{-1}$). Addition of *p*-cresolate as the 18-crown-6-potassium salt in various concentrations (9−30 mM) to the reaction completely inhibited the formation of ethane and $\mathbf{7b_1}$. The rate of C−O coupling in these reactions was independent of the concentration of added aryloxide ($k_{obs} = k_{CO} = (2.1 \pm 0.2) \times 10^{-5}$ s$^{-1}$).

The analogous compounds *fac*-(dppbz)$PtMe_3$(*p*-$OC_6H_4X$) (X = H ($\mathbf{6b_2}$), OMe ($\mathbf{6b_3}$), Cl ($\mathbf{6b_4}$), $CF_3$ ($\mathbf{6b_5}$), CN ($\mathbf{6b_6}$)) were prepared in the same manner as $\mathbf{6b_1}$. Thermolysis of the complexes $\mathbf{6b_{1-6}}$ in THF-$d_8$ at 120 °C in the presence of the appropriate 18-crown-6 potassium aryloxide in each case yielded the anisole product and **2b** in quantitative yield. All thermolyses followed first-order kinetic behavior and the respective rate constants are listed in Table 3. Figure 4 shows a Hammett plot for this reaction, using $\sigma^-$ values.[37−39] The Hammett plot exhibits a good fit with a positive $\rho$ value of 1.44 ($r^2 = 0.986$).

**Scheme 4**

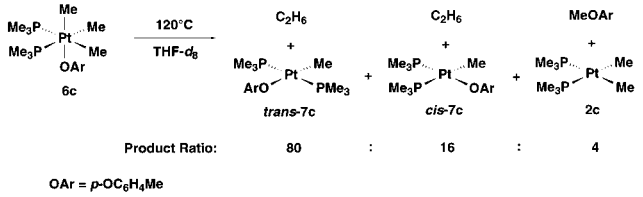


Thus, the reaction is considerably faster for more electron withdrawing substituents ($k_{obs} = 5.6 \times 10^{-4}$ s$^{-1}$ for *p*-CN) than for electron donating substituents ($k_{obs} = 2.1 \times 10^{-5}$ s$^{-1}$ for *p*-Me).

The dppbz complex *fac*-(dppbz)$PtMe_3$(*p*-$OC_6H_4Me$) ($\mathbf{6b_1}$) demonstrates similar behavior to that of the dppe analogue **6a** in the presence of Lewis acids. While in the absence of acid, $k_{obs} = (2.7 \pm 0.2) \times 10^{-5}$ s$^{-1}$, the addition of *p*-cresol brings about a significant acceleration of the reaction ($k_{obs} = 3.2 \times 10^{-4}$ s$^{-1}$, 30 mM, 0.8 equiv). In addition, C−C coupling to form ethane and (dppbz)PtMe(*p*-$OC_6H_4Me$) ($\mathbf{7b_1}$) increases from 15% to 30% of the reaction products ($k_{CO} = 2.2 \times 10^{-4}$ s$^{-1}$ and $k_{CC} = 1.0 \times 10^{-4}$ s$^{-1}$). Thus, acids have a catalytic effect on both the C−O and C−C coupling processes. This is strikingly similar behavior to that observed for the Pt acetate complex *fac*-(dppe)$PtMe_3$(OAc) (**1a**).

Also of note is that the exchange of aryloxides is more rapid and occurs at lower temperatures than reductive elimination for these complexes. When 18-crown-6 potassium phenoxide (6.0 mM, 0.21 equiv) was added to a solution of the platinum *p*-cresolate complex $\mathbf{6b_1}$ (28.2 mM in THF-$d_8$) and the tube heated at 79 °C, complete exchange (formation of an equilibrium mixture of $\mathbf{6b_1}$and $\mathbf{6b_2}$ and the corresponding aryloxide salts) was observed over the course of 20 h.[40] Since exchange is observed at temperatures 40 °C lower than those at which reductive elimination occurs at similar rates (120 °C), aryloxide exchange is considerably faster than the reductive elimination reactions.

**(c) A Monodentate Phosphine Aryloxide Complex of Pt(IV).** The monodentate phosphine complex *fac*-$(PMe_3)_2PtMe_3$-(*p*-$OC_6H_4Me$) (**6c**) was prepared in high yield (91%) by reaction of potassium *p*-cresloate with $[PtMe_3OTf]_4$ followed by the addition of $PMe_3$. When heated at 120 °C in THF-$d_8$, this complex rapidly undergoes reductive elimination to form ethane and a mixture of *cis*- and *trans*-$(PMe_3)_2PtMe(OAr)$ (*cis*- and *trans*-**7c**) in 93% yield (77% cis, 16% trans, Scheme 4). A small amount (ca. 4%) of the C−O coupling products, *p*-methylanisole and *cis*-$(PMe_3)_2PtMe_2$ (**2c**),[41] was observed. The reaction was

(35) (a) Rominger, R. L.; McFarland, J. M.; Jeitler, J. R.; Thompson, J. S.; Atwood, J. D. *J. Coord. Chem.* **1994**, *31*, 7. (b) Morita, D. K.; Stille, J. K.; Norton, J. R. *J. Am. Chem. Soc.* **1995**, *117*, 8576. (c) Garrou, G. E. *Adv. Organomet. Chem* **1984**, *23*, 95 and references therein.

(36) Variable and higher percentages of C−C coupling were observed in the absence of the acid scavenger, PVP.

(37) A wide variety (see refs 37a−c, 38, and 40) of values for $\sigma^-$ for any given substituent is available in the literature. The values reported in ref 37a were used as this represented the most recent and comprehensive source, and the values were exclusively determined by the p$K_a$ of the analogous phenol rather than the anilinium cation (which frequently yields a very different $\sigma^-$ value (ref 37c)). The value for *p*-$CF_3$ was obtained from ref 37b due to its exclusion from ref 37a. (a) Fischer, A.; Leary, G. J.; Topsom, R. D.; Vaughan, J. *J. Chem. Soc. B* **1967**, 846. (b) Liotta, C. L.; Smith, D. F., Jr. *Chem. Commun.* **1968**, *7*, 416. (c) *Correlation Analysis in Chemistry: Recent Advances*; Chapman, N. B., Shorter, J., Eds.; Plenum Press: New York, 1978.

(38) (a) See the following for an excellent early review of Hammett relationships: Jaffé, H. H. *Chem. Rev.* **1953**, *53*, 191. (b) Exner, O. In *Correlation Analysis in Chemistry−Recent Advances*; Chapman, N. B., Shorter, J., Eds.; Plenum Press: New York, 1978; p 439. (c) *Advances in Linear Free-Energy Relationships*; Chapman, N. B., Shorter, J., Eds.; Plenum Press: London, 1972.

(39) Exner, O. *Correlation Analysis of Chemical Data*; Plenum Press: New York, 1988; and references therein.

(40) Overlap of the signals in the NMR spectrum prevented facile quantitative measurement of the equilibrium constant.

(41) Clark, H. C.; Manzer, L. E. *J. Organomet. Chem.* **1973**, *59*, 411.

**Scheme 5**

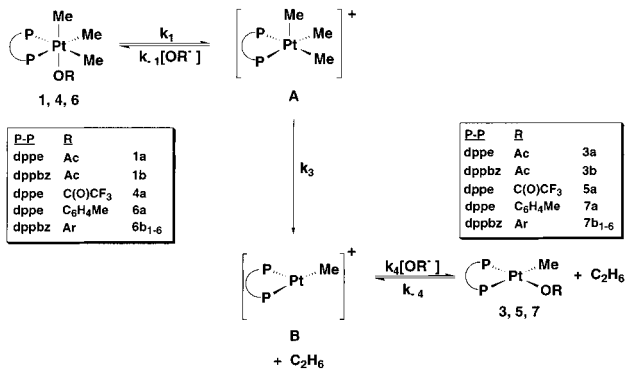


approximately 90% complete in 1 h, but did not exhibit linear first-order kinetic behavior.

When $PMe_3$ was added to the reaction (2 equiv), the disappearance of **6c** followed first-order behavior ($k_{obs} = 7.5 \times 10^{-7}$ s$^{-1}$). More significant is that the rate of ethane formation was slowed by approximately a factor of a 1000 and C−O coupling became competitive. Throughout the reaction, the C−O coupled product *p*-methylanisole was produced in 40% yield.[42]

## Discussion

**Mechanism of Carbon−Carbon Bond Formation.** Carbon−carbon reductive elimination has been observed from a number of Pt(IV) phosphine alkyl complexes. Mechanistic evidence suggests that for all sp$^3$−sp$^3$ carbon−carbon couplings from Pt(IV), dissociation of a ligand occurs prior to reductive coupling.[43−45] For the complexes *fac*-$L_2PtMe_3X$, where L = a monodentate neutral ligand and X = halide or alkyl group, preliminary dissociation of L occurs.[45a,b] For *fac*-$L_2PtMe_3I$ where $L_2$ is the bidentate phosphine dppe, iodide dissociation precedes C−C coupling.[43] Finally, for (dppe)$PtMe_4$, dissociation of one arm of the phosphine chelate occurs prior to C−C coupling.[44] Thus in each case, the C−C coupling reaction takes place from a five-coordinate intermediate. The results of our study of the thermal chemistry of *fac*-$L_2PtMe_3OR$ complexes point to a similar mechanism for the C−C reductive elimination reactions from these compounds.

For *fac*-$L_2PtMe_3OR$ (OR = carboxylate, aryloxide) complexes with bidentate phosphines, the thermally promoted carbon−carbon reductive elimination reaction was completely inhibited by the addition of the conjugate base, $OR^-$. This inhibition points to a mechanism in which carboxylate or aryloxide dissociates prior to the C−C bond forming step (Scheme 5). Ignoring contributions to the rate law from the competitive C−O reductive elimination, the rate constant for C−C coupling can be expressed as $k_{CC} = k_1k_3/(k_{-1}[OR^-] + k_3)$.[46] Thus, as $[OR^-]$ increases, the rate of C−C reductive elimination will approach zero. As expected for a mechanistic pathway involving the generation of ionic intermediates ($L_2PtMe_3^+$ and $OR^-$), the use of more polar solvents has a significant accelerative effect on the rate of C−C coupling from *fac*-$L_2PtMe_3OR$. For example, the rate constant for this reaction increases by approximately 3 orders of magnitude on going from $C_6D_6$ to nitrobenzene-$d_5$ for the thermolysis of *fac*-(dppe)$PtMe_3$(OAc) (**1a**) (Table 2).

The addition of Lewis acids, which can coordinate to OR and assist in $OR^-$ dissociation (increasing $k_1$ and decreasing $k_{-1}$, Scheme 5), would also be expected to accelerate the C−C reductive elimination reaction. The ability of even weak acids to bind to these species is demonstrated by the X-ray crystal structure of the dppe Pt(IV) acetate complex, **1a**, in which a water molecule is hydrogen bound to the acetate moiety (Figure 1). In agreement with this prediction, the addition of small amounts of triflic acid or silver triflate to benzene-$d_6$ solutions of the Pt(IV) trimethyl acetate complex **1a** resulted in very high rates of C−C coupling. The addition of acetic acid produced a somewhat smaller rate acceleration of the C−C reductive elimination (ca. 5×) as the effect was attenuated by the simultaneous addition of the acetate ion. Similar enhancements of the rate of C−C coupling were observed for the *p*-cresolate complexes of dppe (**6a$_1$**) and dppbz (**6b$_1$**) when small amounts of cresol were added to the thermolysis reactions. Finally, it should be noted that carbon−carbon reductive elimination is 2 orders of magnitude more rapid from the trifluoroacetate complex **4a** than from the acetate complex **1a**. As trifluoroacetate is a much better leaving group than acetate, this again supports a mechanism involving dissociation of the $OR^-$ group prior to ethane elimination (Scheme 5).

For *fac*-$L_2PtMe_3X$ (X = halide or methyl) complexes containing monodentate ligands L, evidence has been provided for L dissociation as a preliminary step in the mechanism of C−C reductive elimination.[45a,b] Even in the case of the bidentate phosphine complex, (dppe)$PtMe_4$, there is evidence for the dissociation of one arm of the chelate prior to the C−C coupling step.[44] To probe the importance of preliminary phosphine dissociation in reductive elimination reactions from *fac*-$L_2PtMe_3OR$ complexes, the thermal reactivity of the monodentate phosphine complex *fac*-$(PMe_3)_2PtMe_3(p\text{-}OC_6H_4Me)$ (**6c**) was investigated. Carbon−carbon reductive elimination from **6c** is much faster than from the analogous compounds bearing bidentate ligands; at 120 °C, thermolysis is nearly complete within 1 h. Reductive elimination produces predominantly the C−C coupled products ethane and an equilibrium mixture of *cis*- and *trans*-$(PMe_3)_2PtMe(p\text{-}OC_6H_4Me)$ (*cis*- and *trans*-**7c**) (>90%). This reaction was not first order in the absence of added phosphine. In contrast, addition of ca. 2 equiv of $PMe_3$ greatly inhibits the rate of carbon−carbon reductive elimination and results in first-order kinetic behavior.[47] This inhibition by added phosphine suggests that $PMe_3$ dissociation precedes C−C coupling from **6c**.

The possibility that similar phosphine dissociation is important in the thermolysis of the bidentate phosphine complexes *fac*-$L_2PtMe_3OR$ ($L_2$ = dppe, dppbz) was also considered. However,

(42) Due to overlap of signals, ethane and the platinum products could not be integrated during the progress of the reaction. Unfortunately, the long reaction times (>2 months for the reaction to reach completion) and high temperature (120 °C) caused degradation of the platinum products over time, preventing clear quantification of the products other than the anisole, which was consistently produced in 40% yield throughout the reaction.

(43) (a) Goldberg, K. I.; Yan, J. Y.; Breitung, E. M. *J. Am. Chem. Soc.* **1995**, *117*, 6889. (b) Goldberg, K. I.; Yan, J. Y.; Winter, E. L. *J. Am. Chem. Soc.* **1994**, *116*, 1573.

(44) Crumpton, D. M.; Goldberg, K. I. *J. Am. Chem. Soc.* **2000**, *122*, 962 and references therein.

(45) (a) Brown, M. P.; Puddephatt, R. J.; Upton, C. E. E. *J. Chem. Soc., Dalton Trans.* **1974**, 2457. (b) Roy, S.; Puddephatt, R. J.; Scott, J. D. *J. Chem. Soc., Dalton Trans.* **1989**, 2121. In the absence of added L, 1−2% of C−C reductive elimination from $L_2PtMe_4$ (L = MeNC, 2,6-$Me_2C_6H_3$-NC) may proceed without ligand dissociation. Significant decomposition of L under the reaction conditions hinders complete analysis of the data. (c) Hill, G. S.; Yap, G. P. A.; Puddephatt, R. J. *Organometallics* **1999**, *18*, 1408. (d) Hill, G. S.; Puddephatt, R. J. *Organometallics* **1997**, *16*, 4522.

(46) Note that while the competitive C−O coupling reaction does actually affect the rate law ($k_2$ appears in the denominator; see Conclusions), this inverse dependence of $k_{CC}$ upon $[OR^-]$ remains valid even when the C−O coupling reaction is taken into account.

(47) Note that in the absence of $PMe_3$, only small amounts (<5%) of *p*-methylanisole and *cis*-$(PMe_3)_2PtMe_2$ (**2c**) are produced, while in the presence of added $PMe_3$, the percentage of anisole formed rises to 40%

**Scheme 6**

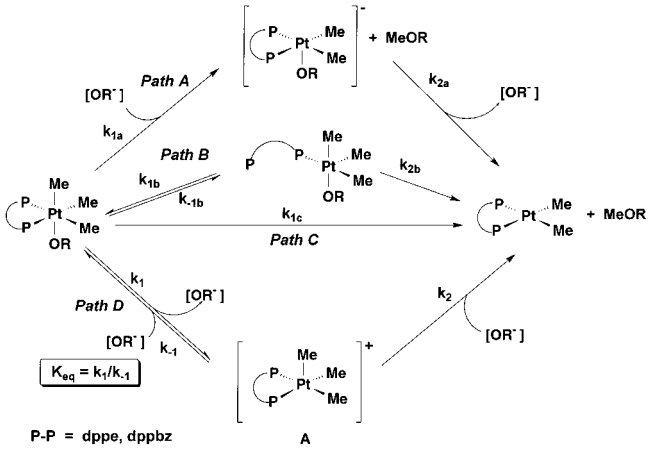


the fact that C−C coupling is completely inhibited in the bidentate cases by the addition of $OR^-$ argues strongly against this proposal. While it is conceivable that $OR^-$ could coordinate to the Pt center after phosphine dissociation, it is highly unlikely that $OR^-$ would be able to compete effectively with recoordination of the pendant phosphine arm. It should be noted that very small concentrations of $OR^-$ were sufficient to completely inhibit C−C coupling; in the case of *fac*-(dppbz)$PtMe_3$(*p*-$OC_6H_4Me$) (**6b$_1$**), no C−C coupling was observed even when [$OAr^-$] was as low as 3 mM. Thus, it seems that in these *fac*-$L_2PtMe_3(OR)$ complexes, phosphine dissociation prior to C−C coupling is the primary mechanism for C−C reductive elimination from those complexes containing monodentate phosphines. However, such phosphine dissociation is essentially unimportant in cases in which the phosphine is bidentate. Instead, $OR^-$ dissociation precedes C−C coupling for these complexes. These results are similar to those found for C−C reductive elimination from the complexes *fac*-$L_2PtMe_3I$ (L = $PMe_2Ph$, $L_2$ = dppe) in which either monodentate phosphine dissociates or iodide dissociates prior to C−C coupling.[43,45a]

**Mechanism of C−O Reductive Elimination.** While reductive elimination reactions to form C−C bonds from platinum(IV) centers are well-known,[43−45] such reactions to form C−O bonds are extremely rare.[17] We have observed and been able to study in detail the mechanisms of C−O reductive elimination from several different Pt(IV) alkyl carboxylate and aryloxide complexes. The C−O reductive elimination reactions from these various complexes share many key elements. For the complexes *fac*-$L_2PtMe_3OR$ ($L_2$ = bidentate phosphine; OR = carboxylate, aryloxide), the C−O coupling reactions are independent of the external concentration of $OR^-$, and are accelerated by more polar solvents and by acids. The carbon−oxygen coupling reactions were also found to be faster for more electron withdrawing R groups. These shared features suggest a common mechanism for C−O reductive elimination from these Pt(IV) carboxylate and aryloxide complexes.

Four different mechanisms for C−O reductive elimination from *fac*-$L_2PtMe_3(OR)$ ($L_2$ = dppe, dppbz) have been considered (Scheme 6). The first of these, Path A, involves direct nucleophilic attack upon the six-coordinate species by $OR^-$. However, such a reaction path would show a first-order kinetic dependence upon $OR^-$ ($k_{obs} = k_{1a}[OR^-]$). The C−O coupling reactions were found to be independent of the concentration of $OR^-$, and thus Path A can be excluded.

The second possible C−O coupling mechanism, Path B, involves preliminary phosphine dissociation to generate a five-coordinate intermediate from which C−O coupling takes place. It was recently reported that C−C reductive elimination from the related bidentate phosphine complexes (dppe)$PtMe_3R$ (R = Me, Et) proceeds via such preliminary phosphine dissociation at 165 °C.[44] In addition, *fac*- and *mer*-(dppe)$PtMe_3Et$ were shown to interconvert at 100 °C on a time scale of hours. Since such isomerizations of Pt(IV) octahedral complexes are generally proposed to occur via five-coordinate intermediates,[48,49] it is likely that dissociation of one end of the dppe chelate is kinetically accessible in the 99 °C carboxylate and 120 °C aryloxide thermolyses. The role of phosphine dissociation (Path B) in C−O coupling from platinum(IV) was investigated by the study of the monodentate phosphine complex *fac*-$(PMe_3)_2$-$PtMe_3$(*p*-$OC_6H_4Me$) (**6c**). Upon thermolysis, this complex was observed to rapidly undergo C−C, not C−O reductive elimination. Appreciable C−O coupling (40%) was observed only when the phosphine dissociation pathway was blocked by addition of $PMe_3$. This demonstrates that while C−O coupling can occur from **6c**, phosphine dissociation is not on the reaction coordinate, and that phosphine loss leads instead to C−C elimination. Additional evidence against preliminary phosphine dissociation in these C−O coupling reactions from Pt(IV) is the similarity in the rate constants of C−O coupling from *fac*-(dppe)$PtMe_3$-(OAc) (**1a**) and *fac*-(dppbz)$PtMe_3$(OAc) (**1b**). Both complexes exhibit a rate constant for C−O reductive elimination of $k_{CO} = 1 \times 10^{-5}\ s^{-1}$. If phosphine dissociation were required to occur prior to the C−O coupling reaction, one would expect that the more rigid dppbz complex would react more slowly. This effect was observed in the investigation of C−C reductive elimination from $L_2PtMe_4$ ($L_2$ = dppe, dppbz), in which the dppbz complex underwent C−C coupling approximately 2 orders of magnitude more slowly than the corresponding dppe complex.[44]

Exclusion of Path A and Path B leaves us to distinguish between the single-step, concerted pathway C and the two-step $OR^-$ dissociation/nucleophilic attack pathway D. A substantial body of evidence suggests that Path D is the more reasonable mechanism. First, C−O coupling from the acetate **1a** is four times faster in acetone-$d_6$ ($4.0 \times 10^{-5}\ s^{-1}$) than in THF-$d_8$ or benzene-$d_6$ ($1.1 \times 10^{-5}\ s^{-1}$). This solvent dependence suggests an ionic or polar transition state.[50] Such a transition state would be expected for Path D, but not for a concerted elimination such as Path C. In addition, C−O coupling from the acetate, **1a**, is accelerated by acetic acid and C−O coupling from the *p*-cresolate complex **6b$_1$** is accelerated by *p*-cresol. The assistance of an acid should promote the dissociation of $OR^-$ from *fac*-$L_2PtMe_3(OR)$ ($K_{eq}$ in Path D, Scheme 6). This would increase the overall reaction rate for Path D, while it is difficult to reconcile such an acceleration with the mechanism shown in Path C.

The rate constants for C−O reductive elimination from the aryloxide complexes **6b$_{1-6}$** were easily measured in the presence of added aryloxide. Under these conditions, C−C coupling was completely inhibited and the rate constants ($k_{CO}$) were shown to be independent of the added aryloxide concentration. A Hammett plot of the rate constants $k_{CO}$ for **6b$_{1-6}$** exhibited a $\rho$ value of 1.44, which demonstrates that the reaction rate increases with more electron withdrawing aryloxides. Note that a similar trend is observed in the carboxylate complexes, in which the platinum(IV) trifluoroacetate complex **4a** undergoes C−O reductive elimination an order of magnitude faster than the

(48) Clark, H. C.; Manzer, L. E. *Inorg. Chem.* **1973**, *12*, 362. (b) Crespo, M.; Puddephatt, R. J. *Organometallics* **1987**, *6*, 2548.

(49) Five-coordinate intermediates have also been proposed in the isomerization of octahedral Ir(III) complexes. Wehman-Ooyevaar, I. C. M.; Drenth, W.; Grove, D. M.; van Koten, G. *Inorg. Chem.* **1993**, *32*, 3347.

(50) Isaacs, N. S. *Physical Organic Chemistry*; John Wiley and Sons: New York, 1987; pp 183−184.

acetate analogue, **1a**. These observations are more consistent with Path D, in which dissociation occurs to form a negative charge at the oxygen, than with Path C.

The absolute magnitude of the $\rho$ value is difficult to predict but a $\rho$ value of 1.44 can be shown to be consistent with Path D by analysis of the rate law for this mechanism. Since C−C reductive elimination is completely inhibited in the presence of added aryloxide, there is no contribution of a C−C coupling path to the rate expression under these conditions. When a steady-state concentration of the intermediate five-coordinate cationic Pt(IV) species (**A**, Scheme 6) is assumed, a first-order rate expression with $k_{obs} = k_1k_2/(k_{-1} + k_2)$ is derived for Path D. However, it was shown that the exchange of aryloxides is significantly more rapid than the C−O reductive elimination reaction. Complete exchange with added aryloxide was observed (i.e., equilibrium was reached) at temperatures much lower than those required for reductive elimination. Thus, the first step of the mechansim depicted in Path D, dissociation of the aryloxide group, should be viewed as a preequilibrium. The second step, nucleophilic attack of the aryloxide on the platinum bound methyl group of intermediate **A**, is then rate limiting and the kinetic expression simplifies to $k_{obs} = (k_1/k_{-1})k_2 = K_{eq}k_2$. Since $k_{obs} = K_{eq}k_2$, $\rho_{obs} = \rho_{eq} + \rho_2$.[51] These constituent $\rho$ values can be crudely estimated from analogous organic reactions. For dissociation of phenols in water at 25 °C, $\rho_{eq}$ has been determined to be 2.113, while nucleophilic attack at $sp^3$ carbon by aryloxides has been shown to exhibit $\rho$ values lying between −0.771 and −0.994.[37c] Thus, a value of ca. 1.2 could be predicted for Path D. While this is a *very* rough estimate (there should be substantial solvent effects in these reactions and the substrates involved are not metal-bound methyl groups), it suggests that a $\rho$ value of 1.44 is at least consistent with such a mechanism.

Thus, the mechanistic evidence provides the strongest support for Path D, a two-step pathway in which the $OR^-$ group dissociates, and then peforms $S_N2$ attack upon a methyl group of the five-coordinate cation **A**. It should also be noted that the second step in Path D, the nucleophilic attack of an oxygen center upon an electrophilic Pt(IV) methyl group, bears a strong resemblance to the proposed final step in the Shilov cycle.[2,3] Labinger and Bercaw have provided convincing evidence that this alcohol formation step proceeds by $S_N2$ attack of water on a Pt(IV) alkyl ligand.[3]

An interesting comparison can be made between this mechanism for C−O reductive elimination from Pt(IV) and that proposed for carbon−heteroatom reductive elimination from Pd(II).[7b,c,12] Reductive elimination reactions to form aryl C−O and C−N bonds serve as the product formation steps in palladium-catalyzed syntheses of aryl ethers and arylamines, respectively.[6−8,12] In contrast to the Pt(IV) reactions, the rates of the Pd(II) reactions increase with increasing nucleophilicity of the heteroatom group. This is because the reactions proceed via a direct intramolecular nucleophilic attack of the heteroatom on the electrophilic hydrocarbyl group.[7b,c,12] Initial dissociation of the heteroatom group prior to coupling is not required. Thus, although directly opposite trends are observed with respect to the electronics of the heteroatom group in these carbon−heteroatom couplings from Pt(IV) and Pd(II), the reactions share a common feature in that the heteroatom group acts as a nucleophile upon a metal-bound carbon.

**Origin of Nonlinear Kinetics in the Thermolysis of *fac*-(dppe)PtMe$_3$(*p*-OC$_6$H$_4$Me) (6a).** It was noted during the thermolysis of *fac*-(dppe)PtMe$_3$(*p*-OC$_6$H$_4$Me) (**6a**) at 120 °C in THF-$d_8$ that the reaction accelerated as time progressed (Figure 2). In addition, the thermolysis of **6a** in the presence of 18-crown-6-potassium aryloxide afforded [18-crown-6-potassium]-[H(OAr)$_2$] and a mixture of *cis*-(PMePh$_2$)(P(CHCH$_2$)Ph$_2$)PtMe$_2$ (**8**), *cis*-(P(CHCH$_2$)Ph$_2$)$_2$PtMe$_2$ (**9**), and *cis*-(PMePh$_2$)$_2$PtMe$_2$ (**10**) as minor products (Scheme 3). Similar decompositions of dppe to vinyl phosphines have been observed in Pd chemistry in the presence of strong bases.[7a,52] When the strong base KOH was allowed to react with *fac*-(dppe)PtMe$_3$(O$_2$CCF$_3$) (**4a**), the same Pt(II) complexes (**8**−**10**) were generated quantitatively.

Since the most acidic protons on the dppe Pt(IV) complexes are those in the phosphine ethyl backbone, initial deprotonation of this site is a likely first step in the degradation. Consistent with this analysis, the complex analogous to **6a** with a phosphine aryl backbone, *fac*-(dppbz)PtMe$_3$(*p*-OC$_6$H$_4$Me) (**6b$_1$**), did not display curvature in first-order kinetic plots of its thermolysis reaction and no signs of phosphine degradation were observed even in the presence of added aryloxide. The degradation of the dppe backbone suggests an explanation for the nonlinear first-order kinetic behavior of *fac*-(dppe)PtMe$_3$(*p*-OC$_6$H$_4$Me) (**6a**). Even in the absence of added aryloxide, there should be a small concentration of aryloxide due to dissociation of aryloxide from **6a**. The resultant Pt(IV) cation would be susceptible to deprotonation by the aryloxide anion. While this cannot be a major reaction (<3%) because the products are not observed by $^1$H or $^{31}$P NMR, even a trace amount of phenol produced in this way would be sufficient to accelerate the reaction and result in non-first-order behavior. Note that the addition of a larger amount of *p*-cresol (0.8 equiv) to the thermolyses of **6a** brought about a much faster reaction, but also resulted in first-order kinetic behavior. Under these conditions, the cresol is present under pseudo-first-order conditions (i.e., the generation of trace amounts of cresol would not change the overall concentration of cresol by an appreciable amount). Similarly, addition of 18-crown-6-potassium aryloxide to the thermolysis of **6a** also resulted in first-order behavior. In this case, the cresol produced is trapped in the form of the bicresolate anion H(OAr)$_2^-$ (observed by $^1$H NMR), which is a much less competent acid catalyst.

## Conclusions

The limited number of model complexes for which studies of C−O reductive elimination involving alkyl carbons from high-valent metal centers could previously be conducted has inhibited the development of a mechanistic understanding of this important C−O coupling reaction. We have observed and carried out detailed investigations of carbon−oxygen reductive elimination reactions from a variety of Pt(IV) complexes of the form *fac*-L$_2$PtMe$_3$(OR) (R = acyl, aryl) (Scheme 7). The C−O reductive elimination reactions to form methyl esters or methyl aryl ethers from these complexes compete in many cases with C−C coupling reactions to form ethane. Our evidence supports two-step mechanisms for both carbon−oxygen and carbon−carbon reductive elimination reactions from the Pt(IV) complexes *fac*-L$_2$PtMe$_3$OR. C−O reductive elimination takes place by preliminary dissociation of $OR^-$ followed by nucleophilic attack of the dissociated $OR^-$ anion on a methyl carbon of the five-coordinate cationic Pt(IV) species. This attack by an oxygen nucleophile upon an electrophilic Pt(IV)-bound methyl group is closely analogous to that proposed to be operative in the Shilov oxidation catalyst.

While C−O coupling proceeds via $OR^-$ dissociation and $S_N2$ attack by $OR^-$ upon a platinum-bound methyl group, carbon−

(51) Reference 39, p 70.

(52) Zhuravel, M. A.; Glueck, D. S. Personal communication.

**Scheme 7**

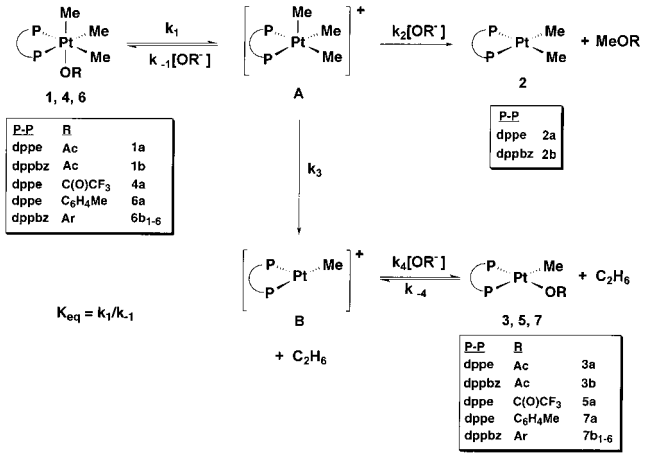


carbon reductive elimination from Pt(IV) proceeds via preliminary dissociation of either a neutral phosphine ligand or $OR^-$ anion followed by C−C coupling from the five-coordinate Pt(IV) intermediate. If phosphine dissociation is limited by the chelate effect, then both C−O and C−C coupling from *fac*-$L_2PtMe_3OR$ (R = acyl, aryl) proceed through the same five-coordinate intermediate as shown in Scheme 7. The overall rate expression for the reaction in Scheme 7 (eq 1) predicts that both C−O and C−C reductive elimination reactions would be facilitated by factors which enhance dissociation of $OR^-$ from the six-coordinate starting material (increase $k_1$ and decrease $k_{-1}$). Thus, the incorporation of electron withdrawing groups into $OR^-$, the addition of Lewis acids, and the use of more polar solvents all increase the rates of both reductive elimination reactions.

$$k_{obs} = \frac{k_1(k_2[OR^-] + k_3)}{(k_{-1} + k_2)[OR^-] + k_3} \qquad (1)$$

Notably, these factors tend to enhance C−C coupling more than C−O coupling. For example, the trifluoroacetate complex **4a** undergoes C−O coupling an order of magnitude faster than the acetate complex **1a**, but the C−C coupling is 2 orders of magnitude faster. Likewise, HOAc (3 mM) causes a 2-fold increase in C−O coupling rate from **1a**, but a 5-fold increase in C−C coupling rate.[53] C−O coupling from **1a** is four times faster in the more polar solvent acetone-$d_6$ than in $C_6D_6$, but C−C coupling is faster by a factor of 100. These results are all consistent with the mechanism shown in Scheme 7. Conditions which enhance $OR^-$ dissociation will have an accelerative effect on C−C reductive elimination because they act to increase $k_1$ and decrease $k_{-1}$. In contrast, while these same factors accelerate the first step of the C−O reductive elimination reaction (increase $k_1$, decrease $k_{-1}$), they act to inhibit the second step, nucleophilic attack by $OR^-$ on a Pt(IV) methyl group (decrease $k_2$).

Choice of reaction conditions can be effectively used to select for either the C−O or C−C coupled product. Since the five-coordinate intermediate **A** (Scheme 7) must choose between C−O coupling, which depends on the nature and the concentration of $OR^-$, and C−C elimination, which is independent of the nature and concentration of $OR^-$, selection for C−O reductive elimination can be favored by the use of nonpolar solvents, more nucleophilic $OR^-$ species, and the addition of $OR^-$ to the reaction. In the presence of added $OR^-$, carbon−carbon coupling is completely inhibited and the rate of carbon−oxygen coupling is independent of the concentration of $OR^-$. Under these conditions, the rate equation simplifies to $k_{obs} = k_{CO} = (k_1/k_{-1})k_2 = K_{eq}k_2$.

Although more nucleophilic $OR^-$ groups favor C−O coupling over C−C coupling, a significant problem was encountered with the use of basic $OR^-$ groups. Since these $OR^-$ groups dissociate from the metal, they can act as competent bases to attack and degrade the ligand. Dppe complexes of the form *fac*-(dppe)-$PtMe_3(OR)$ were found to undergo ligand degradation with the addition of KOH or [18-crown-6-K][OAr] (R = $C(O)CF_3$, Ar) or even upon thermolysis without added base (R = Ar). However, we have also shown that the judicious choice of a ligand which lacks acidic protons (e.g. dppbz) can circumvent the problems posed by basic $OR^-$ groups. This aspect of ligand design must be considered in attempting to use these C−O coupling reactions in metal-mediated organic transformations.

However, a better reason to avoid the use of highly basic $OR^-$ groups may be that despite the fact that carbon−oxygen bond formation requires the action of $OR^-$ as a nucleophile, the reaction is actually accelerated by the use of more electron withdrawing $OR^-$ groups. In other words, *the weaker $OR^-$ is as a nucleophile, the faster the nucleophilic coupling of R′ and OR in the Pt(IV)R′(OR) system.* While this is somewhat counterintuitive, it is a direct result of the unusual two-step mechanism of C−O coupling in these high-valent platinum(IV) species. This implies that the most useful coupling groups in platinum-catalyzed alkane functionalization processes may be sulfonates, trifluoroacetate, or water, rather than halides, hydroxides, acetate, or alkoxides, despite the initially attractive nucleophilicities of the latter species. Indeed, the Shilov catalyst system forms methanol by nucleophilic attack of water on a platinum-bound methyl group[2,3] and the Catalytica system couples a methyl group with bisulfate.[4] The use of sulfonates, trifluoroacetate, and bisulfate to form the C−O coupled products is particularly attractive because these species can protect the alcohol derivative from overoxidation.[3−5] Thus, not only are these among the easiest protecting groups to remove in post-catalysis treatment, they may also be the easiest to attach to the alkyl fragment in the final metal-mediated step.

## Experimental Section

**General Considerations.** Unless otherwise noted, all transformations were carried out under an $N_2$ atmosphere in a drybox, using standard Schlenk techniques, or under vacuum. THF, diethyl ether, benzene, and toluene were distilled under $N_2$ from sodium/benzophenone ketyl. Pentane, methylene chloride, and benzyl ether were distilled from $CaH_2$. Nitrobenzene-$d_5$ was dried over $P_2O_5$ and stored over 4 Å sieves. Acetone was dried over $CaSO_4$ and stored over 4 Å sieves. Deuterated solvents were dried by analogous methods and transferred under vacuum. $PMe_3$ was dried over a sodium mirror. Tetrabutylammonium acetate (Aldrich) was recrystallized from THF/diethyl ether. KH was purchased as a suspension in mineral oil, isolated on a fritted glass funnel, washed repeatedly with hexanes, and dried under vacuum. *o*-Bis-(diphenylphosphino)benzene (dppbz) was purchased from Strem and was either used as provided or treated with KH and recrystallized from THF/pentane. Other reagents, unless specified, were used as received from commercial suppliers. NMR spectra were recorded on Bruker DPX200, AC200, AF300, DRX499, or AM500 spectrometers. All coupling constants are reported in Hz. $^1H$ and $^{13}C$ spectra were referenced by using residual solvent peaks and are reported in ppm

(53) (a) The addition of AgOTf and HOTf shows an even more dramatic trend in acceleration of C−C coupling, but this can be attributed to a special salt effect, in which the silver or proton abstracts the anion, forming the unstable complex *fac*-Pt(dppe)$Me_3$OTf and HOAc or AgOAc. This is different from the analogous reaction with HOAc, in which the exchange reaction is nonproductive, and only the hydrogen bonding or Lewis acid coordination generate reaction acceleration. For more information and leading references on special salt effects, see: March, J. *Advanced Organic Chemistry*, 4th ed.; John Wiley and Sons: New York, 1992; pp 303−304.

downfield of tetramethylsilane. $^{31}$P spectra were referenced to external $H_3PO_4$ (0 ppm). $^{195}$Pt spectra were referenced to external aqueous $K_2PtCl_4$. $^{19}$F spectra were referenced to external $CF_3CO_2H$ and are reported in ppm downfield of $CFCl_3$ ($CF_3CO_2H = -77$ ppm). IR spectra were recorded on a Perkin-Elmer 1720 Infrared Fourier Transform spectrometer at 1 $cm^{-1}$ resolution. Elemental analyses were performed by Canadian Microanalytical Laboratory or Atlantic Microlab. $[PtMe_3I]_4$ and *fac*-(dppe)$PtMe_3I$ were prepared by established literature procedures.[41,54] Cross-linked poly-4-vinylpyridine (PVP, 2%) was purchased from Aldrich, and dried under high vacuum for 12−36 h at temperatures between 100 and 120 °C. Celite was dried for >48 h at >150 °C under vacuum.

**Preparation of *fac*-(dppe)$PtMe_3$(OAc) (1a).** *fac*-(dppe)$PtMe_3I$ (311.2 mg, 0.407 mmol) was suspended in toluene (25 mL) and AgOAc (Aldrich, 99.999%, 77 mg, 0.46 mmol) was added slowly while the solution was stirred vigorously. The colorless solution became yellow and cloudy within minutes, was isolated from light, and was allowed to stir for 13 h. At the end of this time, the yellow silver iodide precipitate was removed by vacuum filtration through Celite on a medium porosity glass fritted funnel. The solution was evaporated to dryness and exposed to air.[55] Cross-linked poly-4-vinylpyridine (PVP, 2%) was added and allowed to stir with the product for 3.5 h, to remove any remaining silver salts. The PVP was removed by gravity filtration through glass wool and the product recrystallized from toluene/*n*-heptane (−25 °C) and washed with pentane (2 crops, 184 mg, 64% yield). $^{31}$P{$^1$H}NMR ($C_6D_6$): $\delta$ 23.0 (s w/Pt satellites, $^1J_{PtP} = 1147$). $^1$H NMR ($C_6D_6$): $\delta$ 0.05 (t w/Pt satellites, 3H, $^2J_{PtH} = 70$, $^3J_{PH} = 7.8$, Pt-C**H**$_3$ trans to O), 1.84 (t w/Pt satellites, 6H, $^2J_{PtH} = 57$, $^3J_{PH} = 6.8$, Pt-C**H**$_3$ cis to O), 1.80 (s, 3H, $PtO_2CC$**H**$_3$), 2.5, 3.3 (both m, 2H each, P-C**H**$_2$-C**H**$_2$-P), 6.9−7.3 (m, protons of phosphine phenyl rings), 7.7−7.8 (t, $J = 8$, 4H, *ortho*-protons of phosphine phenyls proximal to acetate). $^{13}$C{$^1$H} NMR ($C_6D_6$): $\delta$ −9.9 (s w/Pt satellites, $^1J_{PtC} = 632$, Pt-**C**$H_3$ trans to O), 8.2 (dd w/Pt satellites, $^1J_{PtC} = 539$, trans-$^2J_{PC} = 120$, cis-$^2J_{PC} = 5$, Pt-**C**$H_3$ cis to O), 23.5 (s w/Pt satellites, $^3J_{PtC} = 13$, $PtO_2$**C**$CH_3$), 28.4 (complex AA′X pattern, P**C**$H_2$**C**$H_2$P), 126−135 (various aromatic signals for phosphine phenyls, not clearly resolved), 175.7 (s w/Pt satellites, $^2J_{PtC} = 9.5$, Pt-$O_2$**C**$CH_3$). $^{195}$Pt{$^1$H}NMR ($C_6D_6$): 817 (t, $^1J_{PtP} = 1145$). IR($CH_2Cl_2$): $\nu_{CO} = 1377$, 1614 $cm^{-1}$. Anal. Calcd for $C_{31}H_{36}O_2P_2Pt\cdot 0.5(H_2O)$ (706.70): C, 52.69; H, 5.28. Found: C, 52.64; H, 5.09.

**Solution of X-ray Crystal Structure of 1a.** Colorless rhombohedric crystals of **1a**·$H_2O$ were grown by slow evaporation from a toluene solution at ambient temperature on the benchtop. A crystal was mounted on a glass capillary with epoxy and data were collected on an Enraf-Nonius CAD4 diffractometer (Table 4).[20] Solution and refinement were carried out employing XPREP SHELXS and SHELXL provided by Siemens. All hydrogens were located by using a riding model. All non-hydrogen atoms were refined anisotropically by full-matrix least squares.

**Preparation of *fac*-(dppe)$PtMe_3(O_2CCF_3)$ (4a).** *fac*-(dppe)$PtMe_3I\cdot CH_2Cl_2$ (1.131 g, 1.330 mmol) was dissolved in chilled toluene (110 mL, −35 °C), to which was added $Ag(O_2CCF_3)$ (Aldrich, 98% 0.299 g, 1.35 mmol). Yellow precipitate (AgI) immediately became visible, and after ca. 5 min, the reaction mixture was filtered through a fine porosity fritted funnel layered with Celite. The solution was subsequently evaporated to dryness under vacuum, while taking care to isolate the solution from light. The residue was then dissolved in diethyl ether (150 mL), gravity filtered through glass wool, and layered with pentane (100 mL). The solution was cooled to −35 °C and white crystals formed over a 24 h period. The crystals were washed with cold ether and pentane (972.7 mg, 97% yield, 3 crops). $^{31}$P{$^1$H}NMR ($C_6D_6$): $\delta$ 20.7 (s w/Pt satellites, $^1J_{PtP} = 1124$). $^1$H NMR ($C_6D_6$): $\delta$ 0.13 (t w/Pt satellites, 3H, $^2J_{PtH} = 73$, $^3J_{PH} = 7.9$, Pt-C**H**$_3$ trans to O), 1.80 (t w/Pt satellite, 6H, $^2J_{PtH} = 56$, $^3J_{PH} = 6.9$, Pt-C**H**$_3$ cis to O), 2.5, 3.2 (both m, 2H each, P-C**H**$_2$-C**H**$_2$-P), 7.0−7.4 (m protons of phosphine phenyl rings), 7.77 (t, $J = 8$, 4H, *ortho*-protons of phosphine phenyls proximal to trifluoroacetate). $^{13}$C{$^1$H} NMR ($C_6D_6$): $\delta$ −8.2 (s w/Pt satellites, $^1J_{PtC} = 660$, Pt-**C**$H_3$ trans to O), 9.2 (dd w/Pt satellites $^1J_{PtC} = 530$, *trans*-$^2J_{PC} = 114$, *cis*-$^2J_{PC} = 5$, Pt-$CH_3$ cis to O**)**, 27.1 (complex AA′X pattern, $PCH_2CH_2P$), 116.1 (q, $^1J_{CF} = 292$, $CF_3$), 129−133 (various aromatic signals for phosphine phenyls, not clearly resolved), 161.6 (q $^2J_{CF} = 35$, Pt-$O_2CCF_3$). $^{195}$Pt{$^1$H} NMR ($C_6D_6$): $\delta$ 895 (t, $^1J_{PtP} = 1125$). $^{19}$F NMR ($C_6D_6$): $\delta$ −74 (br s).

**Table 4.** Crystal Structure Information for *fac*-(dppe)$PtMe_3$(OAc)·$H_2O$ (**1a**·$H_2O$)

| | |
|---|---|
| empirical formula | $C_{31}H_{38}O_3P_2Pt$ |
| formula weight | 715.64 |
| temperature (K) | 183(2) |
| wavelength (Å) | 0.71073 |
| crystal system | triclinic |
| space group | $P\bar{1}$ (No. 2) |
| unit cell dimensions | |
| $a$ (Å) | 10.048(2) |
| $b$ (Å) | 12.581(3) |
| $c$ (Å) | 13.538(3) |
| α (deg) | 66.15(2) |
| $\beta$ (deg) | 70.32(2) |
| $\gamma$ (deg) | 78.16(2) |
| vol (Å$^3$) | 1469.1(6) |
| $Z$ | 2 |
| calcd density (Mg $m^{-3}$) | 1.618 |
| abs coeff ($mm^{-1}$) | 4.914 |
| $F$(000) | 712 |
| crystal description | colorless rhombahedron |
| crystal size (mm) | 0.35 × 0.30 × 0.25 |
| $\theta$ range for data collection (deg) | 1.72 to 24.97 |
| index ranges | $-11 \le h \le 11$<br>$-14 \le k \le 14$<br>$-15 \le l \le 16$ |
| reflcns collected/unique reflcns | 5444/5119 [$R_{int} = 0.0394$] |
| completion to $\theta = 24.97$ | 99.7% |
| abs correction | Ψ scans |
| refinement method | full-matrix least squares on $F^2$ |
| data/restraints/parameters | 5119/0/334 |
| goodness-of-fit on $F^2$ | 1.075 |
| $R_1$ ($I > 2\sigma(I)$) | 0.0341 |
| $wR_2$[a] (all data) | 0.0995 |
| largest diff peak and hole (e·Å$^3$) | 2.167 and −1.515 |

[a] $w = 1/[\sigma^2(F_o^2) + (0.0802P)^2 + 0.1789P]$, where $P = (F_o^2 + 2F_c^2)/3$.

**Preparation of *fac*-(dppbz)$PtMe_3$(OAc) (1b).** $[PtMe_3I]_4$ (295.6 mg, 0.201 mmol) was dissolved in a minimum of THF (25 mL) and AgOAc (169.8 mg, 1.02 mmol) was added with vigorous stirring. The reaction was isolated from light and stirred overnight. The next day, the yellow AgI precipitate was filtered away through Celite on a glass wool pipet. The solvent was removed from resultant colorless solution under vacuum. The solid residue was redissolved in THF (10 mL) and dppbz (380.7 mg, 0.852 mmol) was added. This reaction was allowed to stir overnight. The volatiles were removed from the yellow reaction mixture under vacuum and the resulting solids triturated three times with 2 mL of toluene. The resultant ivory powder was recrystallized from THF/pentane at −35 °C to afford a white powder that was washed with pentane (1 crop, 551.6 mg, 84% yield as **1b**·THF). $^{31}$P{$^1$H}NMR (THF-$d_8$): $\delta$ 26.4 (s w/Pt satellites, $^1J_{PtP} = 1147$). $^1$H NMR ($C_6D_6$): $\delta$ −0.55 (t w/Pt satellites, 3H, $^2J_{PtH} = 70.0$, $^3J_{PH} = 7.6$, Pt-C**H**$_3$ trans to acetate), 1.16 (t w/Pt satellites, 6H, $^2J_{PtH} = 57.2$, $^3J_{PH} = 7.1$, Pt-C**H**$_3$ cis to acetate), 1.32 (s, 3H, $PtO_2CC$**H**$_3$), 7.0−8.0 (m, protons phosphine aryl rings, unresolved). Anal. Calcd for $C_{35}H_{36}O_3P_2Pt\cdot C_4H_8O$ (745.69): C, 57.28; H, 5.42. Found: C, 57.00; H, 5.14.

**Preparation of *fac*-(dppe)$PtMe_3$(*p*-$OC_6H_4$Me) (6a).** In the drybox, one Schlenk flask was charged with *fac*-(dppe)$PtMe_3(O_2CCF_3)$ (**4a**) (166.1 mg, 0.221 mmol) and THF (5 mL) and a second with potassium *p*-cresolate (98.0 mg, 0.670 mmol) and THF (5 mL). The flasks were capped with septa, brought out of the drybox, and attached to a Schlenk line. The solution of **4a** was cooled to −78 °C, and the potassium salt solution was added slowly via cannula. The reaction mixture was allowed to stir overnight and gradually warmed as the dry ice−acetone bath thawed, warming to room temperature. The solvent was removed

(54) Appleton, T. G.; Bennett, M. A.; Tomkins, B. *J. Chem. Soc., Dalton Trans.* **1976**, 439.

(55) **1a** was prepared both by rigorously anhydrous conditions and as described here, and no difference was observed in the thermolysis rates or product ratios. In all cases, **1a** was recrystallized from anhydrous toluene/pentane under $N_2$ before use in kinetics experiments.

under vacuum, and the product extracted with 55 mL of toluene in the drybox. This suspension was filtered and the solution layered with pentane (65 mL) and cooled to −35 °C. The next day, the crystals were washed with pentane and isolated as a toluene monosolvate (150.6 mg, 81% yield, 2 crops). $^{31}P\{^1H\}$ NMR(THF-$d_8$): $\delta$ 12.9 (s w/Pt satellites, $^1J_{PtP} = 1116$). $^1H$ NMR (THF-$d_8$): $\delta$ 0.19 (t w/Pt satellites, 3H, $^2J_{PtH} = 68.8$, $^3J_{PH} = 7.2$, methyl group trans to O), 1.15 (t w/Pt satellites, 6H, $^2J_{PtH} = 58.8$, $^3J_{PH} = 7.6$, methyl groups trans to P), 2.10 (s, 3H, aryloxide methyl group), 2.8 (4H, m, PC**H**$_2$C**H**$_2$P), 6.10 (2H, d, $^3J_{HH} = 8$, aryloxide C-**H** *ortho* to O), 6.60 (2H, d, $^3J_{HH} = 8$, aryloxide C-**H** *meta* to O), 7−7.5 (complex unresolved aryl signals due to dppe phenyl groups), 7.97 (t, 4H, $^3J_{PH} \sim {}^3J_{HH} = 9$, *ortho* protons on phosphine phenyls proximal to aryloxide). $^{13}C\{^1H\}$ (THF-$d_8$): $\delta$ −10.3 (s w/Pt satellites, $^1J_{PtC} = 631$, methyl trans to O), 6.8 (dd w/Pt satellites, $^1J_{PtC} = 552$, *trans*-$^2J_{PC} = 118$, *cis*-$^2J_{PC} = 5$, methyl groups cis to O), 21.0 (s, aryloxide methyl group), 27 (m, second-order coupling pattern due to phosphine coupling, PC**H**$_2$C**H**$_2$P), 121.6 (s, aryloxide carbon *para* to O), 129.0−129.5 (unresolved m, carbons *meta* to O on phosphine phenyls and carbons *meta* to Pt on aryloxide), 131.1 (unresolved s, *para* carbons on phosphine phenyls), 133.3 (m, phosphine *ortho* carbons distal to aryloxide), 135.6 (m, phosphine *ortho* carbons proximal to aryloxide), 164.3 (s, aryloxide carbon *ipso* to O). The $^{13}C$ spectrum was assigned on the basis of DEPT and 2D correlational spectroscopy. An elemental analysis sample was obtained by grinding the resultant product and storing the compound under vacuum for one week. Anal. Calcd for $C_{36}H_{40}OP_2Pt$ (745.77): C, 57.98; H, 5.41. Found: C, 57.61; H, 5.35.

**Preparation of [PtMe$_3$(OTf)]$_4$.** The literature preparation[21f] was modified as follows: $[PtMe_3I]_4$ (856.2 mg, 0.583 mmol) was dissolved in THF (15 mL), to which AgOTf (Aldrich, 99%, 785.4 mg, 3.057 mmol) was added. Yellow precipitate (AgI) formed instantly, and after five minutes of stirring, the suspension was gravity filtered four times through glass wool. The solvent was removed under vacuum, and the product was recrystallized first from THF/pentane, then from THF/ether. The crystals obtained were washed with THF and ether, and dried under vacuum overnight (3 crops, 876.8 mg, 97% yield). NMR data matched those reported in the literature.[21f]

**Preparation of Aryloxide Salts.** Aryloxide salts of potassium (*p*-$KOC_6H_4X$) were obtained by reaction of the appropriate phenol (purchased from Aldrich and used as received) with KH (in excess, 1.5−3 equiv) overnight in THF. The solution was filtered through glass wool to remove excess KH, and the potassium salts recrystallized from THF/diethyl ether at −35 °C. The 18-crown-6-potassium aryloxides were prepared by reaction of the potassium aryloxide with 18-crown-6 (Aldrich) and KH in THF overnight. After filtering the solutions to remove the excess KH and evaporating them to dryness, the products were recrystallized from THF/ether at −35 °C.

**Preparation of *fac*-(dppbz)PtMe$_3$(*p*-OC$_6$H$_4$X) (6b$_{1-6}$).** All of the aryloxide complexes of dppbz (X = Me (**6b$_1$**), H (**6b$_2$**), OMe (**6b$_3$**), Cl (**6b$_4$**), $CF_3$ (**6b$_5$**), CN (**6b$_6$**)) were prepared in an analogous fashion. The preparation of the parent phenoxide compound is provided as typical. $[PtMe_3(OTf)]_4$ (125 mg, 0.0807 mmol) was dissolved in THF (10 mL). KOPh (43.0 mg, 0.325 mmol) was added and a colorless crystalline material (KOTf) became evident within a few minutes. The next day, the solution was gravity filtered through Celite on glass wool to afford a colorless solution. Dppbz (147.6 mg, 0.324 mmol) was then added, and the solution turned pale yellow. After ca. 24 h, more THF was added (40 mL total), and the product solution was filtered through glass wool. The solution was layered with pentane (100 mL) and cooled to −35 °C. After 4 days, yellowish crystals were collected, washed with pentane, and dried under vacuum (190.3 mg, 76% yield). These crystals were recrystallized a second time from toluene/pentane before use in kinetic studies, at which time white crystals were obtained. NMR data for all aryloxide compounds are provided in Table 5. NMR signals were assigned as indicated in Figure 5 on the basis of 2D correlational spectroscopy. Yields: **6b$_1$**, 76%; **6b$_2$**, 70%; **6b$_3$**, 63%; **6b$_4$**, 56%; **6b$_5$**, 60%; **6b$_6$**, 70%. IR for **6b$_6$**: $\nu_{CN} = 2204$ cm$^{-1}$. Anal. Calcd for $C_{40}H_{40}OP_2Pt\cdot 0.5(C_4H_8O)$ (**6b$_1$**·0.5THF, 825.83): C, 61.05; H, 5.36. Found: C, 61.09; H, 5.53. Anal. Calcd for $C_{39}H_{38}OP_2Pt$ (**6b$_2$**, 779.76): C, 60.07; H, 4.92. Found: C, 60.21; H, 4.92. Anal. Calcd for $C_{39}H_{37}ClOP_2Pt$ (**6b$_4$**, 814.20): C, 57.53; H, 4.58. Found: C, 57.85; H, 4.71. Anal. Calcd for $C_{40}H_{37}F_3OP_2Pt$ (**6b$_5$**, 847.75): C, 56.67; H, 4.47. Found: C, 56.78; H, 4.40. Anal. Calcd for $C_{40}H_{37}NOP_2Pt$ (**6b$_6$**, 779.76): C, 59.70; H, 4.63; N, 1.72. Found: C, 59.37; H, 4.78; N, 1.74.

**Table 5.** NMR Data for *fac*-(dppbz)PtMe$_3$(*p*-OC$_6$H$_4$X) (**6b$_{1-6}$**)

| | | **6b$_1$** *p*-H | **6b$_2$** *p*-Me | **6b$_3$** *p*-OMe | **6b$_4$** *p*-Cl | **6b$_5$** *p*-$CF_3$ | **6b$_6$** *p*-CN |
|---|---|---|---|---|---|---|---|
| $^{31}P$ NMR | $\delta$ | 23.0 | 22.5 | 22.3 | 23.2 | 24.3 | 25.0 |
| | $^1J_{PtP}$ | 1135 | 1139 | 1143 | 1143 | 1140 | 1142 |
| $^1H$ NMR | | | | | | | |
| $Me_a$ | $\delta$ | −0.27 | −0.30 | −0.31 | −0.25 | −0.19 | −0.10 |
| | $^2J_{PtH}$ | 70.0 | 69.5 | 68.5 | 70.4 | 71.2 | 71.4 |
| | $^3J_{PH}$ | 7.0 | 6.7 | 7.0 | 7.0 | 7.0 | 7.0 |
| $Me_b$ | $\delta$ | 1.25 | 1.22 | 1.17 | 1.21 | 1.27 | 1.31 |
| | $^2J_{PtH}$ | 59.0 | 59.0 | 58.0 | 58.8 | 58.8 | 57.5 |
| | $^3J_{PH}$ | 7.6 | 7.7 | 7.5 | 7.7 | 7.8 | 7.5 |
| OAr | $\delta$(H2) | 6.30 | 6.22 | 6.22 | 6.23 | 6.35 | 6.34 |
| | $^3J_{HH}$ | 8.5 | 8.0 | 8.5 | 8.8 | 8.6 | 8.5 |
| | $\delta$(H3) | 6.81 | 6.63 | 6.45 | 6.76 | 7.09 | 7.14 |
| | $^3J_{HH}$ | 7.80 | 8.00 | 8.50 | 9.00 | n/a | 8.50 |
| | $\delta$(X) | 6.24[b] | 2.11 | 3.59 | n/a | −59.50[a] | n/a |
| backbone | $\delta$ (H6) | 7.55 | 7.53 | 7.58 | 7.60 | 7.59 | 7.59 |
| Ph | $\delta$ (H7) | 7.59 | 7.57 | 7.58 | 7.63 | 7.62 | 7.59 |
| $Ph_+$ | $\delta$ (H9) | 7.13 | 7.11 | 7.18 | 7.16 | 7.13 | 7.1 |
| | $\delta$ (H10) | 7.33 | 7.2 | 7.2 | 7.38 | 7.36 | 7.33 |
| | $\delta$ (H11) | 7.33 | 7.2 | 7.2 | 7.38 | 7.36 | 7.33 |
| $Ph_-$ | $\delta$ (H13) | 7.96 | 7.99 | 8.05 | 7.95 | 7.84 | 7.78 |
| | *J*(H13) triplet | 8.6 | 8.7 | 9 | 8.8 | 8.9 | 9.2 |
| | $\delta$ (H14) | 7.26 | 7.2 | 7.2 | 7.32 | 7.36 | 7.26 |
| | *J*(H14) triplet | n/a | n/a | n/a | 7.0 | n/a | 7.0 |
| | $\delta$ (H15) | 7.14 | 7.31 | 7.43 | 7.45 | 7.41 | 7.39 |
| | *J*(H15) triplet | 7.3 | 7 | 7.2 | 7.5 | n/a | 7.5 |
| $^{13}C$ NMR | | | | | | | |
| $Me_a$ | $\delta$ | −6.5 | −6.3 | −7 | −6.5 | −5.4 | −4.9 |
| | $^1J_{PtC}$ | 635 | 635 | 637 | 645 | 714 | 649 |
| $Me_b$ | $\delta$ | 6.3 | 7 | 7.1 | 6.1 | 6.6 | 6.4 |
| | $^1J_{PtC}$ | 548 | 555 | 551 | 546 | 549 | 544 |
| | $^2J_{PC}$(trans) | 113 | 116 | 114 | 115 | 112 | 115 |
| | $^2J_{PC}$(cis) | 5 | 5 | 4 | 5 | 5 | 4 |
| OAr | $\delta$(C1) | 166.4 | 164.0 | 160.0 | 164.7 | 170.1 | 171.3 |
| | $\delta$(C2) | 122.6 | 122.5 | 122.5 | 122.9 | 121.7 | 122.6 |
| | $\delta$(C3) | 128.5 | 129.4 | 114.1 | 128.0 | 126.0 | 133.7 |
| | $\delta$(C4) | 133.3 | 121.4 | 150.1 | 117.0 | 114.6[c] | 95.5 |
| | $\delta$(X) | n/a | 20.6 | 55.5 | n/a | n/a | 121.8 |
| backbone | $\delta$(C5) | 142.8 | 143.2 | 143.3 | 142.4 | 142.7 | 142.6 |
| Ph | $\delta$(C6) | 136.6 | 135.9 | 136.6 | 136.1 | 136.7 | 136.9 |
| | $\delta$(C7) | 132.5 | 132.3 | 132.4 | 133.1 | 133.0 | 133.2 |
| $Ph_+$ | $\delta$(C9) | 133.5 | 133.2 | 133.3 | 133.1 | 133.7 | 133.8 |
| | $\delta$(C10) | 129.0 | 129.1 | 128.7 | 128.5 | 129.2 | 129.3 |
| | $\delta$(C11) | 130.7 | 131.0 | 130.6 | 130.5 | 131.2 | 131.3 |
| $Ph_-$ | $\delta$(C13) | 136.2 | 136.4 | 136.0 | 135.5 | 135.9 | 135.9 |
| | $\delta$(C14) | 128.9 | 129.1 | 128.7 | 128.5 | 129.2 | 129.3 |
| | $\delta$(C15) | 131.5 | 131.4 | 131.0 | 130.9 | 131.6 | 131.8 |

[a] $^{19}F$ NMR. [b] $^3J_{XH_3} = 7.0$ Hz. [c] *q*, $^2J_{CF} = 32$ Hz.

**Preparation of *fac*-(PMe$_3$)$_2$PtMe$_3$(*p*-OC$_6$H$_4$Me) (6c).** $[PtMe_3(OTf)]_4$ (126.5 mg, 0.0813 mmol) and potassium *p*-cresolate (49.2 mg, 0.336 mmol) were combined in THF (10 mL) and allowed to stir overnight. The flask was attached to a stopcock adapter, and the volume was reduced to 5 mL on the vacuum line. $PMe_3$ (1.2 mmol) was added via a known volume bulb (assuming ideal gas behavior, $P = 125$ mmHg). The solution was allowed to stir for 2 h, and then evaporated to dryness and returned to the drybox. The product was taken up in 15 mL of toluene and filtered through Celite on glass wool. This solution was reduced under vacuum to 5 mL and layered with pentane (15 mL). White, feathery crystals were obtained by cooling the layered solution to −35 °C (148.0 mg, 2 crops, 91% yield). $^{31}P\{^1H\}$ NMR (THF-$d_8$): $\delta$ −35.3 (s w/Pt satellites, $^1J_{PtP} = 1290$). $^1H$ NMR (THF-$d_8$): $\delta$ 0.24 (t w/Pt satellites, 3H, $^2J_{PtC} = 69.5$, $^3J_{PH} = 7.5$, methyl group trans to O), 0.73 (approximate dd w/Pt satellites, 6H, $^2J_{PtH} = 55.0$, $^3J_{PH} = 7.5$, $^3J_{P'H} = 6.5$, methyl groups cis to O), 1.41 (second-order $A_9XX'$ pattern, major coupling = 9.0, 18H, P(C**H**$_3$)$_3$), 2.08 (s, 3H, aryl-C**H**$_3$), 6.27 (d, 2H, $^3J_{HH} = 8.5$), aryl C**H** *ortho* to platinum), 6.61 (d, $^3J_{HH} = 8.0$, aryl C**H** *meta* to platinum). Anal. Calcd for $C_{16}H_{34}OP_2Pt$ (499.47): C, 38.48; H, 6.86. Found: C, 38.21; H, 6.82.

**General Treatment of Kinetics Samples.** In the drybox, solid reagents (e.g., platinum complexes, $[NBu_4][OAc]$, PVP, etc.) and benzyl

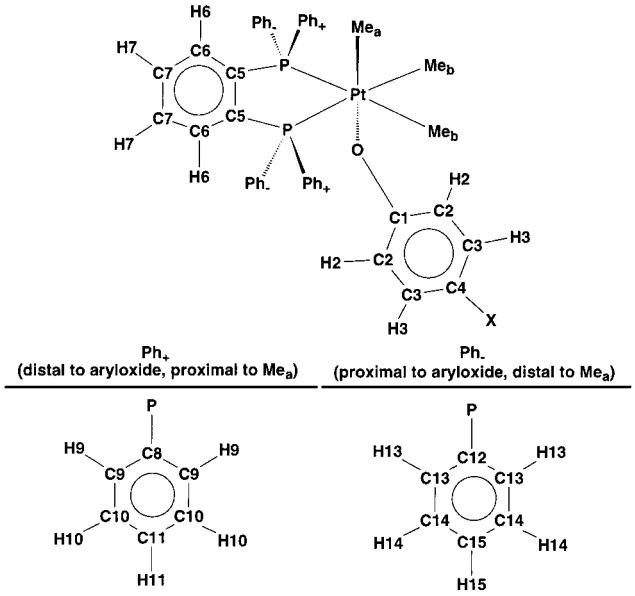


**Figure 5.** Atom labeling scheme for **6b**$_{1-6}$.

ether (an internal standard) were loaded into a medium-walled NMR tube (Wilmad 504) that had been sealed onto a 14/20 joint. The tube was affixed to a stopcock adaptor and evacuated under high vacuum. Solvent was then vacuum transferred into the NMR tube, and the tube was sealed under active vacuum. Nitrobenzene-$d_5$ was transferred at elevated temperature due to low volatility.

NMR tubes were heated in a Neslab Exacal EX-250 HT elevated temperature bath, and the reaction was quenched by rapidly cooling the tube in water (25 °C) or ice water (0 °C). Kinetics tubes were stored in liquid nitrogen when not being actively monitored. All kinetics were performed on DPX200 or DRX499 spectrometers, averaging the integrals of three separate acquisitions for each point. Reactions were followed by the disappearance of the axial methyl group of the Pt(IV) *fac*-$L_2PtMe_3X$ complex relative to benzyl ether ($T_1 = 6$ s, pulses spaced 30 s apart), bis-trimethylsilyl ether ($T_1 = 8$ s, pulses spaced 40 s apart), or ferrocene ($T_1 = 50$ s, pulses spaced 300 s apart) as an internal standard. In all cases, the kinetics samples were followed for 3 half-lives (ca. 10 points) and a rate constant was obtained by a least-squares linear regression method. Kinetics tubes were subsequently heated to completion ($> 7t_{1/2}$) and mass balance was confirmed by integration of products against the internal standard. In cases in which PVP was used, the $^1$H NMR spectrum showed no signs of PVP decomposition or presence in solution.

**Thermolysis of *fac*-(PMe$_3$)PtMe$_3$(*p*-OC$_6$H$_4$Me) (6c) in the Presence of PMe$_3$.** A sealable NMR tube was charged with *fac*-$(PMe_3)_2$-$PtMe_3$(*p*-$OC_6H_4Me$) (5.4 mg, 0.011 mol), THF-$d_8$ (435 $\mu$L), and a drop of benzyl ether as an internal standard. $PMe_3$ (0.022 mmol assuming ideal gas behavior, $P = 24.0$ mmHg) was added by vacuum transfer using a known volume bulb. The disappearance of the proton signals for the aryloxide protons *ortho* to platinum in **6c** was monitored by NMR. However, observation of the platinum-containing products was complicated by the fact that $PMe_3$ exchanges with some of the Pt(II) products, causing line broadening. After the kinetics run, the NMR tube was heated for a further 40 days (70 days ($7t_{1/2}$) total) at 120 °C. The NMR tube was then cracked on the vacuum line and the volatiles collected in another NMR tube, which was then sealed. THF-$d_8$ was then transferred into the original NMR tube, which was then resealed. This allowed clear observation of the products. The reaction conducted in the absence of $PMe_3$ was performed as a typical kinetics experiment (see above). $^{31}$P NMR data for *trans*-$(PMe_3)_2PtMe(OC_6H_4Me)$ (*trans*-**16c**) (THF-$d_8$): $\delta$ −8.9 (s w/Pt satellites, $^1J_{PtP} = 2888$). $^1$H NMR: $\delta$ 0.25 (t w/Pt satellites, Pt-C**H**$_3$, $^2J_{PtH} = 79.0$, $^3J_{PH} = 6.7$), 1.28 (virtual t w/Pt satellites, P(C**H**$_3$)$_3$, $^2J_{PH} = 3.8$, $^3J_{PtH} = 29.5$), 2.09 (s, methyl of aryloxide), 6.66 (s, aryl protons all chemical shift coincident). $^{31}$P NMR data for *cis*-$(PMe_3)_2PtMe(OC_6H_4Me)$ (*cis*-**16c**) (THF-$d_8$): $\delta$ -32.9 (s w/Pt satellites, $^1J_{PtP} = 3697$, **P** trans to OAr), −5.9 (s w/Pt satellites, $^1J_{PtP} = 1699$, **P** trans to Me). $^1$H NMR: $\delta$ 0.41 (dd w/Pt satellites, Pt-C**H**$_3$, $^2J_{PtH} = 54.0$, $^3J_{PH} = 6.7$, $^3J_{P'H} = 4.0$), 1.34 (d w/Pt satellites, P(C**H**$_3$)$_3$ trans to C, $^2J_{PH} = 9.0$, $^3J_{PtH} = 15.5$), 1.60 (d w/Pt satellites, P(C**H**$_3$)$_3$ trans to O, $^2J_{PH} = 10.5$, $^3J_{PtH} = 40.5$), 2.09 (s, methyl of aryloxide), 6.53 (d, protons of aryloxide *ortho* to Pt, $^3J_{HH} = 8.0$), 6.64 (d, protons of aryloxide *meta* to Pt, $^3J_{HH} = 8.5$).

**Reaction of *fac*-(dppe)PtMe$_3$(O$_2$CCF$_3$) (4a) with KOH.** In the drybox, a round-bottomed flask was charged with **4a** (25.1 mg, 0.0334 mmol), KOH (59.5 mg, 1.06 mmol), and THF (5 mL). An aliquot was placed in an NMR tube and the reaction was followed by $^{31}$P NMR. **8** was produced as the primary initial product, with **9** and **10** gaining intensity as the reaction progressed, eventually reaching the 2:1:1 statistical distribution. After allowing the reaction to stir for 1 day, the solvent was removed from the bulk reaction under vacuum, and the solids were dissolved in $C_6D_6$. The products could be unambiguously assigned as a statistical (2:1:1) mixture of *cis*-$(P(CHCH_2)Ph_2)(PMePh_2)$-$PtMe_2$ (**8**), *cis*-$(P(CHCH_2)Ph_2)_2PtMe_2$ (**9**), and *cis*-$(PMePh_2)_2PtMe_2$ (**10**) on the basis of a $^1$H/$^1$H COSY experiment (200 MHz), $^1$H {$^{31}$P}, $^{31}$P-{$^1$H}, and $^1$H experiments at both 200 and 500 MHz, and a long-range (optimized for 7 Hz coupling) $^1$H/$^{31}$P correlation experiment (200 MHz). As further confirmation, dppe was added in large excess to the reaction products, and both $^1$H and $^{31}$P NMR spectra matched those of authentic samples of $(dppe)PtMe_2$ (**2a**), $P(CHCH_2)Ph_2$, and $PMePh_2$ in a 1:1:1 mixture.

**Aryloxide Exchange Experiment.** Both *fac*-(dppbz)PtMe$_3$(*p*-OC$_6$H$_4$-Me) (**6b$_1$**) (9.4 mg, 0.012 mmol) and 18-crown-6-potassium phenoxide (1.0 mg, 0.0025 mmol) were weighed into an NMR tube. On a vacuum line, THF-$d_8$ (420$\mu$L) was added by vacuum transfer, and the tube was sealed. The reaction was heated at 79 °C for 20 h and monitored by $^1$H and $^{31}$P NMR.

**Acknowledgment** is made to the donors of the Petroleum Research Fund, administered by the American Chemical Society, the National Science Foundation, the Union Carbide Innovation Recognition Program, and the DuPont Educational Aid program for support of this work. K.I.G. is an Alfred P. Sloan Research Fellow. We thank J. Roth and A. W. Holland for preliminary work on this project and Prof. J. Mayer for helpful discussions. The X-ray structure determination was performed by Dr. D. Barnhart, S. Lovell, and Dr. W. Kaminsky (UW).

**Supporting Information Available:** Tables of atom coordinates, thermal parameters, hydrogen atom parameters, bond distances, and angles for complex **1a**·$H_2O$ (9 pages, print/PDF). This information is available free of charge via the Internet at http://pubs.acs.org

JA003366K